

# Review on patient-cooperative control strategies for upper-limb rehabilitation exoskeletons

Stefano Dalla Gasperina<sup>1,\*</sup>, Loris Roveda<sup>2</sup>, Alessandra Pedrocchi<sup>1</sup>,  
Francesco Braghin<sup>3</sup> and Marta Gandolla<sup>3</sup>

<sup>1</sup> *NearLab, Department of Electronics, Information and Bioengineering, Politecnico di Milano, Milan, Italy*

<sup>2</sup> *Istituto Dalle Molle di studi sull'Intelligenza Artificiale (IDSIA), USI-SUPSI, Lugano, Switzerland*

<sup>3</sup> *Department of Mechanical Engineering, Politecnico di Milano, Milan, Italy*

Correspondence\*:

Stefano Dalla Gasperina  
stefano.dallagasperina@polimi.it

## 2 ABSTRACT

3 Technology-supported rehabilitation therapy for neurological patients has gained increasing  
4 interest since the last decades. The literature agrees that the goal of robots should be to induce  
5 motor plasticity in subjects undergoing rehabilitation treatment by providing the patients with  
6 repetitive, intensive, and task-oriented treatment. As a key element, robot controllers should  
7 adapt to patients' status and recovery stage. Thus, the design of effective training modalities and  
8 their hardware implementation play a crucial role in robot-assisted rehabilitation and strongly  
9 influence the treatment outcome. The objective of this paper is to provide a multi-disciplinary  
10 vision of patient-cooperative control strategies for upper-limb rehabilitation exoskeletons to  
11 help researchers bridge the gap between human motor control aspects, desired rehabilitation  
12 training modalities, and their hardware implementations. To this aim, we propose a three-level  
13 classification based on i) "high-level" training modalities, ii) "low-level" control strategies, and iii)  
14 "hardware-level" implementation. Then, we provide examples of literature upper-limb exoskeletons  
15 to show how the three levels of implementation have been combined to obtain a given high-level  
16 behavior, which is specifically designed to promote motor relearning during the rehabilitation  
17 treatment. Finally, we emphasize the need for the development of compliant control strategies,  
18 based on the collaboration between the exoskeleton and the wearer, we report the key findings  
19 to promote the desired physical human-robot interaction for neurorehabilitation, and we provide  
20 insights and suggestions for future works.

21 **Keywords:** upper-limb, exoskeleton, rehabilitation, cooperative control, compliant control, human-robot interaction, motor recovery

## 1 INTRODUCTION

22 When recovering from a traumatic event affecting the ability to perform everyday tasks, the primary  
23 goal is to regain functional movements, both at the lower limbs (e.g., walking) and upper limbs (i.e.,  
24 interacting with daily-life objects). The recovery of motor functionalities is usually possible and relatively  
25 straightforward when the traumatic event has an orthopedic source. Still, it becomes trivial when the  
26 traumatic event has a neurological basis, for example, after stroke (Cieza et al., 2020). The outcome of the  
27 rehabilitation treatment strongly depends on some general neurophysiological aspects of motor relearning.  
28 Studies demonstrated that crucial features are high-intensity treatment, repetitive training, involvement and  
29 engagement of the patient, and personalization of the therapy according to the user's residual capability  
30 (Langhorne et al., 2009). Given the increasing burden of neurorehabilitation for therapists and the healthcare  
31 system, exoskeletons have been proposed since the 90s as a suitable support for post-stroke rehabilitation.  
32 Technology-supported therapy aims to provide post-stroke patients with mechatronic devices that help them  
33 perform rehabilitation exercises that can potentially foster motor plasticity and improve motor recovery. The  
34 efficacy of robot-supported interventions has been widely investigated with randomized clinical trials (RCT)  
35 as compared to conventional therapy, and scientific literature reports controversial results (Rodgers et al.,  
36 2019; Mehrholz, 2019). Instead, recent systematic reviews and meta-analyses confirmed the suitability of  
37 the approach to help patients and therapists during the treatment, showing that the use of robotic devices can  
38 positively affect the recovery of arm function in patients with stroke (Veerbeek et al., 2017; Bertani et al.,  
39 2017; Wu et al., 2021). A focus on the clinical outcomes of robot-assisted rehabilitation is not the aim of  
40 this paper. However, looking at the characteristics of a successful rehabilitation program, if well designed,  
41 exoskeletons can provide high-intensity treatment and repetitive training. When coming to the direct  
42 involvement of the patient in the control loop (or human-robot interaction strategy) and the personalization  
43 of the therapy according to the user's residual capability, these are important key features, which are still  
44 under investigation by the scientific community. Overall, robot-mediated rehabilitation therapy should  
45 mimic the quality of conventional therapy performed by physiotherapists and assist patients in regaining lost  
46 functions through a wide selection of training modalities. Moreover, it should adapt to patients' status and  
47 recovery stage, both throughout the single movement and over the rehabilitation treatment (Marchal-Crespo  
48 and Reinkensmeyer, 2009). In addition, there is a great effort in the scientific community to develop  
49 frameworks that take advantage of non-invasive and portable brain monitor techniques (e.g., EEG Noda  
50 et al. (2012); Nicolas-Alonso and Gomez-Gil (2012), fNIRS Hong et al. (2020); Khan et al. (2021)). Such  
51 approaches are employed to detect user intention (i.e., brain-machine interface) and to directly evaluate  
52 motor recovery in terms of neural plasticity, making the framework even more complex. In this work, we  
53 will concentrate on upper limbs recovery and assistance, focusing on control solutions for upper-limb  
54 exoskeletons - based on physical human-robot interaction - and their hardware implementation.

### 55 1.1 Upper-limb exoskeletons and human-robot interaction

56 Upper-limb exoskeletons for rehabilitation have been developed to guide patients in accomplishing  
57 functional tasks as human-like as possible to foster brain plasticity towards recovery. Exoskeleton solutions  
58 that actively guide motion usually consist of serial-connected links that are actuated by powered joints. The  
59 exoskeleton and the user are interconnected through one or more interaction ports, generally represented  
60 by ergonomic cuffs. At the interaction ports level, the exoskeleton and the user exchange forces and  
61 torques. The process by which the human and the robot interact and exchange effort is usually referred to  
62 as physical human-robot interaction. First-generation devices were characterized by rigid movements of  
63 human segments along a prescribed trajectory, thus resulting in the exoskeleton applying forces/torques  
64 at the interaction ports to guide the motion, independently from the effort generated by the user. Thus,  
65 one of the critical advancements in robot-assisted research is describing and harmonizing the relationship

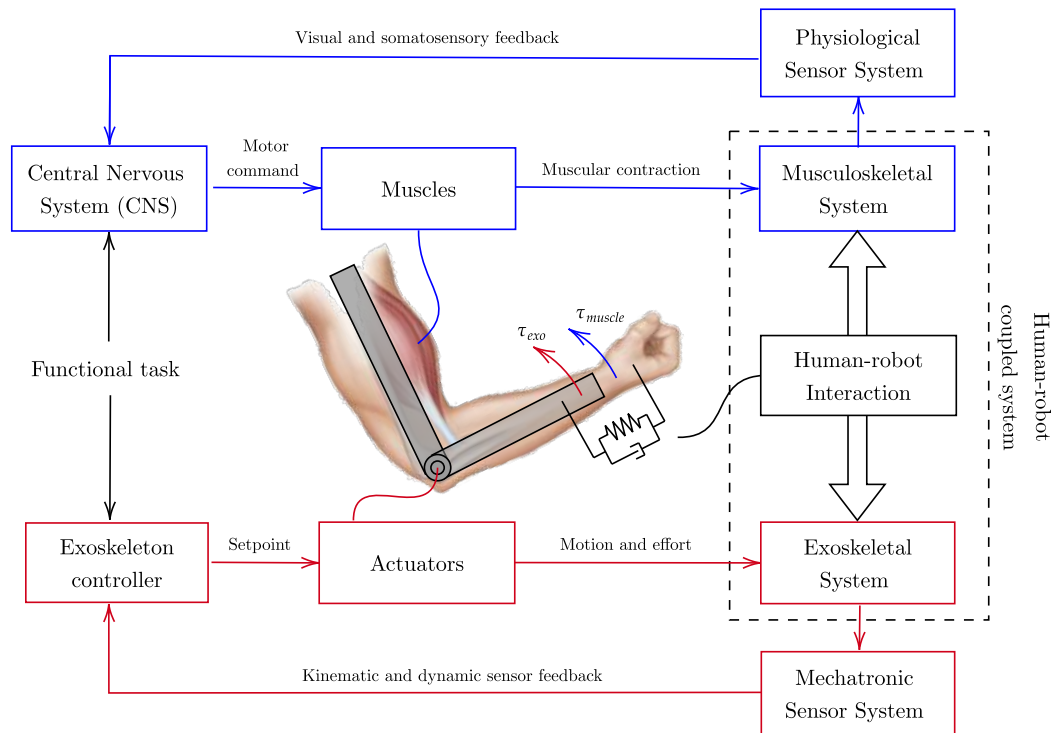


**Figure 1.** Human-robot interaction representation. The blue scheme represents human motor control, and the red scheme refers to the exoskeleton control. The human-robot coupled system cooperates towards the completion of a shared functional task.

66 between voluntary human activity and robot assistance. In fact, robot-assisted movements involved during  
 67 rehabilitation are characterized by two interactive processes, for which we propose the outline represented  
 68 in Figure 1. The first process consists of the patient that is encouraged and tries to perform a functional  
 69 movement, while the latter regards the robot (or the therapist) applying external forces to the patient's arm  
 70 to assist and correct the movement (Kahn et al., 2006a).

71 To complete a functional task, from the human physiological perspective, the intention of the movement  
 72 is elaborated by the Central Nervous System (CNS), which is in charge of delivering appropriate messages  
 73 to manage movement execution through its actuating port, and namely the muscles. During movement  
 74 execution, visual and somatosensory systems provide feedbacks that the CNS analyzes to adjust and  
 75 correct the strategy according to the comparison between the original intention and the effectively executed  
 76 movement. The motor control theory is itself an active field of research, and there is discussion whether  
 77 this comparison is performed accordingly to errors detected at the somatosensory (Gandolla et al., 2014)  
 78 or kinematic level (Krakauer, 2006), which are two sides of the same coin. Similarly, by mimicking the  
 79 human motor control scheme, the exoskeleton controller cooperates with the human by superimposing  
 80 to the muscular effort the (external) robotic contribution, and by shaping the relationship between the  
 81 human motion and the robot assistance. Regardless of the selected control strategy, the aim is to support the  
 82 desired motion as revealed by physical human-robot interaction. The control scheme corrects for kinematic  
 83 or dynamic errors and modulates the set-point signals operated by the mechatronic system's actuators.  
 84 During the motion, the muscle-generated torque ( $\tau_{muscle}$ ) interacts with the actuator-generated torque  
 85 ( $\tau_{exo}$ ), leading to an interactive human-robot coupled system.

## 86 1.2 Related works

87 The rehabilitation process can be divided into three main stages according to time past from the traumatic  
88 event, namely acute, sub-acute and chronic phases (Proietti et al., 2016). Generally, the acute phase  
89 refers to the first week(s) after the injury. The sub-acute phase includes the range between 15-30 and  
90 180 days after the initial stroke (Péter et al., 2011). The chronic phase is instead defined as the open-  
91 ended period starting at about 180 days after initial stroke and characterized by generally slow or no  
92 clinical progress (Bernhardt et al., 2017). During these phases, the rehabilitation treatment should make  
93 the patient progressively regain the range of motion and muscular strength of the injured limb, and the  
94 robot-mediated control strategy should adapt accordingly. In particular, in the earliest stage, since the  
95 patient has lost most of the arm functionalities, the robot should help the patient track a predefined  
96 trajectory to improve the limb range of motion and reduce muscular atrophy or tendon retractions. Recent  
97 studies demonstrated that patients undergoing early robot-mediated therapy within the first weeks after  
98 the trauma could gain greater reductions in motor impairment and improvements in functional recovery  
99 of the upper-limb (Masiero et al., 2007). As soon as the patient has regained some voluntary muscular  
100 contractions, but the generated strength is not adequate to perform precise and complete movements and  
101 consequently not sufficient to fulfill functional tasks, the robot should provide the assistance needed to  
102 complete the movement, as a physical therapist would do. Moreover, to engage the patient and better  
103 induce neural plasticity, the robot should encourage the users to initiate the movements with their active  
104 muscular efforts and progressively provide decreasing assistance until the patient has regained the lost  
105 functionalities. In fact, it has been demonstrated that the carryover effect is selectively obtained when the  
106 patient program the movement and perceives the external assistance as a part of their control loop (Gandolla  
107 et al., 2016b). Finally, when stroke survivors have regained most of the range of motion they could recover,  
108 the robot should help them recover muscle strength. Recent works demonstrated that improvement in motor  
109 function was possible even at late chronic stages, i.e., after the 3-6 months critical window (Ballester et al.,  
110 2019; Gandolla et al., 2021). In this situation, the patient actively performs the exercises against resistive  
111 forces provided by the robot. Further, challenging strategies can be used to involve and engage the users  
112 to continue the rehabilitation treatment. There also exists a branch of robot-assisted rehabilitation that  
113 involves other therapeutic approaches combined with upper-limb exoskeletons. For example, Functional  
114 Electrical Stimulation (FES) has been used to enhance functional recovery of the paretic arm in stroke  
115 survivors (Howlett et al., 2015). The action of FES, combined with the residual voluntary effort of the user,  
116 has proven to enhance cortical plasticity (Gandolla et al., 2016b). For example, Ambrosini et al. (2021)  
117 demonstrated that EMG-triggered FES combined with anti-gravity robotic assistance could improve the  
118 therapeutic effects post-stroke rehabilitation. However, these approaches involve a third interactive process,  
119 i.e., the FES-induced muscular contraction, that must be integrated with the robot controller and the user's  
120 voluntary actions. For this reason, we will not include in detail FES-based robot-mediated rehabilitation  
121 in this work. Overall, it is clear that the design of effective training modalities plays a crucial role in  
122 robot-assisted rehabilitation and strongly influences the treatment outcome.

123 While several reviews on upper-limb exoskeletons are available, most of them deal with the mechanical  
124 design of the robotic systems Lo and Xie (2012); Van Delden et al. (2012); Brackenridge et al. (2016);  
125 Iandolo et al. (2019); Gull et al. (2020) or with their efficacy in clinical practice Maciejasz et al. (2014);  
126 Rehmat et al. (2018). Other reviews investigate robot-mediated rehabilitation control strategies, but they  
127 propose taxonomies and classification that are not consistent, and they typically present control methods at  
128 high-level of implementation Marchal-Crespo and Reinkensmeyer (2009); Basteris et al. (2014); Proietti  
129 et al. (2016); Miao et al. (2018). In particular, with "high-level" strategies, the literature usually refers

130 to those control methods that shape the human-robot interaction behavior and focus on specific training  
131 modalities.

132 For instance, Marchal-Crespo and colleagues presented a review on robotic training strategies Marchal-  
133 Crespo and Reinkensmeyer (2009). The authors specifically target the review to "high-level" strategies,  
134 i.e., such "aspects of the control algorithm that are explicitly designed to provoke motor plasticity". Their  
135 work mainly focuses on assistive controllers classified as i) impedance-based, ii) counterbalance, and iii)  
136 EMG-based methods. According to the authors, the impedance-based controllers create restoring forces  
137 when the participant deviates from the desired exercise trajectory, but they do not intervene if the subject  
138 is moving along the desired path. Counterbalancing controllers, instead, provide weight compensation  
139 to the upper-limb through passive elastic elements or active control schemes, but they do not help the  
140 participant follow the task trajectory. Finally, EMG-based controllers involve surface electromyography  
141 signals (sEMG), and they are aimed at enhancing the residual muscular torques of the participant.

142 In a different recent systematic review, Basteris et al. Basteris et al. (2014) focused on training modalities  
143 in robot-mediated upper-limb rehabilitation and they proposed a classification framework based on the  
144 expected subject's status during human-robot interaction. In their work, training modalities are divided  
145 in four macro categories: i) active, ii) active-assistive, iii) passive, and iii) resistive. In active mode, the  
146 robot does not apply force to the subject's limb and behaves compliantly with the user's movements. In  
147 active-assistive mode, it provides assistance towards the completion of the task. In contrast, in passive  
148 mode, the robot performs the movement without accounting for the subject's activity, while in resistive  
149 mode, it provides forces opposed to the movement. The authors also underline that the literature lacks  
150 information regarding the implementation of the different modalities by different research groups.

151 Another example of review regarding upper-limb exoskeleton control strategies has been proposed by  
152 Proietti and colleagues Proietti et al. (2016). The authors presented a taxonomy based on three main global  
153 rehabilitation features: i) assistance, ii) correction, and iii) resistance. While assistance refers to the ability  
154 of the robot to support the weight of the limb and provide forces to complete the task, with correction  
155 strategies, the robot does not assist the patient, but it corrects the movement to follow a desired path and  
156 to provide coordination among joints. Finally, resistance concerns the robot acting against the desired  
157 movement. However, the authors state that such features are often combined to properly render the desired  
158 human-robot interaction.

### 159 **1.3 Aim of the review**

160 At this stage, it is clear that different research groups presented different taxonomies and classifications,  
161 which are not consistent among works. One of the most challenging aspects of reviewing control strategies  
162 for rehabilitation exoskeletons is to provide the understanding of the control method, which most of the  
163 time is embodied in nested control algorithms and strongly depends on the available robot hardware. In fact,  
164 none of the reviews presented in the literature spans from "high-level" training modalities, to "low-level"  
165 control scheme implementation, to "hardware-level" implementation, to the characterization of the needed  
166 sensor systems, and they do not provide a match between these aspects. The objective of this review is to  
167 provide a multi-disciplinary vision of patient-cooperative control algorithms for upper-limb rehabilitation  
168 exoskeletons. The aim is to bridge the gap between human motor control aspects, rehabilitation training  
169 modalities, and robot development. To this aim, we propose a three-level classification (Table 1). The first  
170 level deals with literature high-level human-robot interaction training modalities, which directly relate  
171 to the desired behavior of the rehabilitation exercise and to the capability of the robotic exoskeleton to  
172 induce motor recovery according to the patients' status. Such high-level modalities are in turn embodied by  
173 low-level control strategies, which promote a large variety of physical human-robot interaction according

Term	Description
"High-level" training modalities	Control strategy that does not necessarily depend on the developed hardware. Directly relates to the desired human-robot interaction behavior during the rehabilitation exercise. Explicitly designed to induce motor plasticity according to the stage of the recover process, and to improve the treatment outcome.
"Low-level" control strategies	Control strategy that depends on the developed hardware. Baseline control law that represents a substrate for implementing a variety of "high-level" modalities. Relates to the capability to promote shared, cooperative, compliant motion between the subject and the robot.
"Hardware-level" implementation	Hardware implementation and control approaches used to promote transparency and compliant motion. Relates to actuation, transmission and sensor technologies involved in the development of compliant joints for rehabilitation exoskeletons.

**Table 1.** Presented classification of control methods for patient-cooperative compliant robotics for upper-limb rehabilitation.

174 to the residual capabilities of the user. Thus, in the second level, we focus on low-level control schemes  
 175 that are exploited to promote compliant motion and to display the desired human-robot behavior. Instead,  
 176 in the third level, namely hardware-level, we draw some insights regarding the state-of-the-art hardware  
 177 implementation, mainly focusing on actuation, transmission and sensor system technologies. Finally, we  
 178 outline how different research groups could achieve the desired physical human-robot interaction with their  
 179 developed hardware. To this aim, we review some upper-limb exoskeleton works as examples of possible  
 180 different choices made at the three proposed levels. Indeed, to promote the desired human-robot interaction  
 181 behavior, different approaches can be followed at different levels of implementation.

## 2 HIGH-LEVEL REHABILITATION TRAINING MODALITIES

182 High-level training modalities have been proposed to promote motor recovery at different stages of the  
 183 rehabilitation treatment, taking inspiration from neuroplasticity and neurophysiological aspects that are  
 184 explicitly involved during motor relearning after stroke (Krakauer, 2006; Reinkensmeyer et al., 2016).  
 185 What researchers want to achieve is to maximize the outcome of the rehabilitation by actively involving the  
 186 patient in the process and by minimizing the robot effort needed for the completion of the rehabilitation task.  
 187 To cope with this objective, the robots should cooperate with the subjects during the treatment as a therapist  
 188 would do. High-level training modalities are usually classified according to the physical interaction between  
 189 the subject and the robot during the rehabilitation training. Thus, most researchers relate rehabilitation  
 190 modalities to the subject's status and engagement (Marchal-Crespo and Reinkensmeyer, 2009; Basteris  
 191 et al., 2014; Trigili et al., 2020), others to the robot's behavior (Pirondini et al., 2016). However, each  
 192 research group presents a different classification, which leads to non-coherent and misaligned literature  
 193 taxonomy. In this review, we posit that upper-limb exoskeletons for rehabilitation can mainly operate in four  
 194 macro-modalities: i) passive, ii) active-assistive, iii) active, and iv) resistive, according to the human-robot  
 195 interaction behavior, which are summarized in Table 2.

## 196 2.1 Passive modalities

197 One of the first approaches used in neurorehabilitation regards passive mobilization of the patient's limb  
198 along a desired trajectory (Lum et al., 2006). The term "passive" refers to the subject's interaction status,  
199 by which the exoskeleton is "active" and performs the movement without accounting for the subject's  
200 intention of action. The robot provides stiff behavior and applies high corrective forces to follow the  
201 desired trajectory (Marchal-Crespo and Reinkensmeyer, 2009). However, passive mobilization has been  
202 proven to limit one of the most important mechanisms of motor relearning: it prevents participants to  
203 program in advance the movement, thus it limits the capability to learn from their mistakes, which are  
204 driving signals for motor learning (Shadmehr et al., 2010). In fact, the CNS creates an internal model of  
205 the environmental dynamics and, during human motor adaptation, it learns to anticipate the movement  
206 according to somatosensory and kinematic errors. (Emken et al., 2007b; Patton et al., 2006). In a clinical  
207 setting, passive mobilization is usually only operated during the first stages of motor recovery. The rationale  
208 of early mobilization is that passive stretching of the limb can prevent stiffening of soft tissue and it  
209 helps to reduce spasticity and tendon retractions (Masiero et al., 2007). Moreover, repetitive movements  
210 of the limb can generate somatosensory stimulation that can potentially induce brain plasticity and help  
211 patients re-learn the desired muscular activation patterns (Bastian, 2008; Crespo and Reinkensmeyer, 2008).  
212 Different variants of passive mode are present in literature.

### 213 2.1.1 Passive-triggered mode

214 The passive-triggered mode consists in the wearer that triggers the exoskeleton assistance as in passive  
215 mode (Proietti et al., 2016). This encourages the participant to self-initiate movements, which is an essential  
216 feature for motor relearning (Marchal-Crespo and Reinkensmeyer, 2009). The trigger can derive from both  
217 cognitive or physical human-machine interfaces. On the one hand, participants can initiate the movement by  
218 means of movement intention detection that can be performed by means of gaze-tracking systems (Novak  
219 and Riener, 2013; Frisoli et al., 2012), Motor Imagery based Brain Computer Interface (MI-BCI) (Barsotti  
220 et al., 2015; Brauchle et al., 2015), or tongue-based interfaces (Ostadabbas et al., 2016). Alternatively, the  
221 passive assistance can be triggered by allowing the participants to attempt a movement with their residual  
222 muscular force (i.e., without any robotic support) and initiate the movement after some performance  
223 conditions are met. In particular, the movement can be triggered by spatial trajectory tracking errors (Kahn  
224 et al., 2006b), movement speed (Krebs et al., 2003), residual forces of the participant (Chang et al., 2007;  
225 Colombo et al., 2005) or EMG-based intention detection (Dipietro et al., 2005; Gandolla et al., 2016a). We  
226 underline that the triggered assistance is generally applied to passive mobilization of the arm, but it can be  
227 also applied to controllers that apply different levels of assistance and resistance to support the arm motion,  
228 such as active-assistive controllers.

### 229 2.1.2 Teach-and-replay mode

230 Different methods exist to define the reference trajectories to be followed by the robot in passive mode. In  
231 teach-and-replay mode, joint trajectories are created by recording the robot joint angles during a teaching  
232 phase. In this phase, the robot is generally operated in transparent mode (the controller compensates for  
233 the robot weight and dynamics) not to resist external forces and to undergo external motion. The therapist  
234 guides the affected arm in the workspace, and the desired trajectory is recorded from the exoskeleton  
235 joints. In some approaches, relevant way-points are determined, and the trajectory is optimized through a  
236 minimum-jerk algorithm to avoid undesired oscillations and achieve natural human-like movements (Nef  
237 et al., 2007; Lin et al., 2021). Then, the robot actively performs the task taught by the therapist, replays  
238 the joint trajectories, and corrects trajectory deviations with corrective gains (Kumar et al., 2019). The  
239 therapist can usually tune the execution velocity of the task to match the patient's needs (Nef et al., 2007;

240 Xu et al., 2011). When the desired movement is registered apriori by the contralateral arm (i.e., the healthy  
241 one), this modality can also be addressed as record-and-replay mode (Proietti et al., 2016).

### 242 2.1.3 Passive-mirrored mode

243 A different option is the passive-mirrored mode, which can be implemented only with exoskeletons  
244 provided with two arms (Van Delden et al., 2012). The strategy consists of passively mimicking the  
245 behavior of the healthy limb by supporting the impaired one passively (Proietti et al., 2016). Usually, this  
246 mode can also be referred to as "master-slave" mode since the desired trajectory is continuously computed  
247 and commanded by its contralateral side, which is generally operated to behave transparently to the healthy  
248 limb (Colizzi et al., 2009; Kumar et al., 2019).

## 249 2.2 Active-assistive modalities

250 Since passive controllers do not involve active participation from the patient, the literature suggests that  
251 more complex control strategies based on subject's involvement could lead to better results, at least after  
252 the first stages of the rehabilitation process (Huang and Krakauer, 2009; Reinkensmeyer et al., 2016).  
253 This is the case of assistive controllers, by which participants are involved in the completion of the task,  
254 while the robot partially assist them in the completion of the task. Due to their nature, assistive strategies  
255 guarantee compliant interaction between the human and the robot, and they permit deviation from the  
256 desired trajectory (if it exists). As previously mentioned, this feature is a key concept for motor learning as  
257 it preserves patients motivation and self-esteem while forcing them to actively adapt their internal models to  
258 minimize kinematic tracking errors (Krakauer, 2006; Shadmehr et al., 2010). Similarly to what introduced  
259 by Marchal-Crespo and Reinkensmeyer (2009), we further divide active-assistive modalities in two different  
260 groups: (i) weight counterbalance assistance, which introduces an offset compensation that counterbalances  
261 the weight of the arm; (ii) trajectory-based corrective assistance, which generates a force-field environment  
262 that helps the user follow the desired trajectory, and (iii) inter-joints coordination assistance, which  
263 regulates the coordination of the joints and promotes physiological synergies during trajectory-based  
264 and free movements. From a more control-based perspective, active-assistive modalities can thus be  
265 implemented through a feedback loop combined with a feedforward contribution, as shown in Figure  
266 2. The feedback closed-loop regulates the position or the interaction forces along the reference exercise  
267 trajectory (i.e., impedance-based correction), while the feedforward loop compensates for perturbation  
268 with a model-based prediction, such as weight counterbalance assistance and friction compensation.

269 On top of this general control scheme, several additional features can be added to achieve inter-joint  
270 coordination, to implement mirror-based or teach-and-play strategies, or to adapt the assistance according  
271 to the treatment outcome. Most exoskeleton prototypes can be operated by a combination of these features.

### 272 2.2.1 Weight counterbalance assistance

273 In the first case the robot provides the effort only to compensate for weak muscular tone that is unable  
274 to support the weight of the arm. In purely counterbalancing strategies, there is no trajectory tracking  
275 correction, and the user can actively explore the range of motion. Weight counterbalance is usually  
276 implemented through feedforward compensation of the arm weight and dynamics. Several anti-gravity  
277 compensation algorithms are available in literature. Most methods are based on dynamic models of the  
278 robot-patient system (Just et al., 2017). To compensate for the robot dynamics, its mechanical properties  
279 (masses, centers of mass and inertia tensors of each joint-link) are usually extracted from the CAD model of  
280 the robotic system (Nef et al., 2007; Just et al., 2016), while weights and lengths of the human arm can be  
281 derived from literature anthropometric tables, such as (Winter, 2009). Once the dynamic properties of the  
282 two interacting systems are obtained, they are fed in to geometric (Moubarak et al., 2010), Lagrangian (Nef  
283 et al., 2007) or recursive (Kim and Deshpande, 2017) inverse-dynamics algorithms to compute the desired

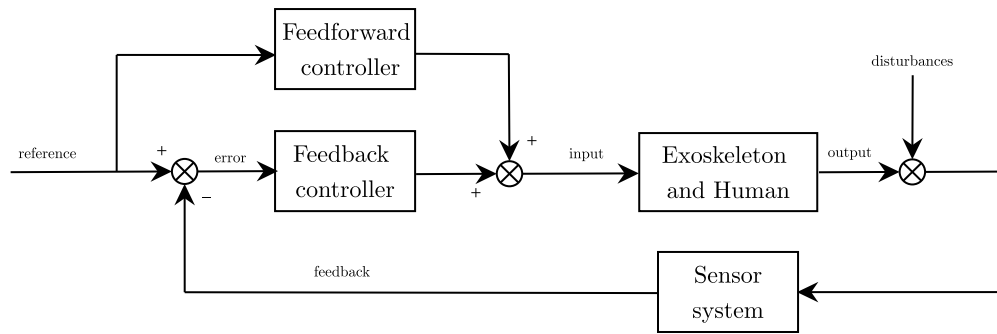


**Figure 2.** General control scheme. Feedback control (impedance-based corrective assistance) and feedforward control (counterbalance assistance) sum up to compute the desired control input.

284 joint torques to compensate for the gravity of the human-robot system. However, mathematical models do  
 285 not always entail a real experience of weight relief for the end-user, and methods to compensate for inertia  
 286 and load uncertainties have been developed for safe and accurate control of upper-limb exoskeletons. For  
 287 instance, Wang and Barry (2021) developed a  $H_\infty$  robust adaptive controller that can adapt to the inertia  
 288 and load uncertainties and compensate for their effects. In a simulation study, the authors proved that such  
 289 adaptive controllers could be applied to safe and reliable motion control of rehabilitation exoskeletons.  
 290 Other approaches are instead based on measurements from force-interfaces (Ragonesi et al., 2013; Just  
 291 et al., 2020), and combine the experimental data to accurately identify the gravity term without extracting  
 292 mass and inertia parameters (Moubarak et al., 2010).

293 Yet another solution to the weight balancing problem is using passive elastic elements to generate  
 294 additional torques to counterbalance gravity. For instance, the RETRAINER (Ambrosini et al., 2017;  
 295 Puchinger et al., 2018) employs passive springs to compensate for the wearer weight. Other examples, such  
 296 as the Pneu-WREX (Sanchez et al., 2005; Wolbrecht et al., 2008) or the BLUE SABINO exoskeletons  
 297 (Perry et al., 2018; Hill et al., 2019), employ elastic elements in combination with active controllers.

### 298 2.2.2 Trajectory-based corrective assistance

299 In trajectory-based corrective strategies, the user has to follow a desired trajectory and the robot corrects  
 300 undesired behavior, similarly to a position control system, but with a more compliant behavior (Marchal-  
 301 Crespo and Reinkensmeyer, 2009). The exoskeleton usually does not intervene as long as the patient is  
 302 following the correct movement. In fact, to accommodate human variability in performing movement,  
 303 a deadband is usually introduced where the user can move freely. Outside the deadband, if the subject  
 304 deviates from the target trajectory, the system produces a gradient of restoring forces that usually vary  
 305 proportional to the trajectory deviation (Nef et al., 2007). Despite the low-level control strategy, the robot  
 306 is usually commanded to recover from kinematic errors through a virtual zeroth order impedance (i.e.,  
 307 a spring), namely implementing pure stiffness control. The controller implements a corrective action or  
 308 force-field to guide the user along a desired trajectory or path. By relaxing the corrective gains of the  
 309 exoskeleton (i.e., by lowering the virtual stiffness), the system displays a more compliant behavior. More  
 310 recent upper-limb exoskeletons include also corrective controllers provided with viscous force-fields that  
 311 dampen and stabilize the movements (Proietti et al., 2015; Kim and Deshpande, 2017).

### 312 2.2.3 Inter-joint coordination assistance

313 Jarrassé et al. (2014) presented a review of studies on upper-limb coordination in stroke patients, intending  
314 to illustrate the potential of robotic exoskeletons to rehabilitate inter-joint coordination. Usually, inter-  
315 joint coordination can be addressed as a kinematic problem that promotes the activation of physiological  
316 muscular synergies compromised by the stroke event. However, most training strategies focus on supporting  
317 all the joints of the exoskeletons independently. Very few approaches have attempted to address the spatio-  
318 temporal relationship between joints, and the clinical efficacy of this approach is still questionable (Jarrassé  
319 et al., 2014). Since most active-assistive controllers follow a reference trajectory, one of the simplest ways  
320 to promote inter-joint coordination is to generate a set of joint trajectories that respect specific coordination  
321 and time-dependency among them. However, computing such joint trajectories is a significant issue. They  
322 can be recorded from physiological movements performed by healthy subjects, or the therapist can guide  
323 them in a teach-and-replay fashion, or they can be computed through optimal inter-joint coordination  
324 inverse-kinematics planners. However, these approaches still require programming specific movements  
325 in advance and need to be re-computed for each task or exercise. Consequently, they limit the patients'  
326 freedom of movement with the exoskeleton, and they do not investigate the inter-joint coordination problem  
327 as a whole.

328 For instance, Brokaw et al. (2013) developed a Time Independent Functional Training (TIFT) method that  
329 provides focused training of inter-joint coordination after stroke and permits movement only if a good level  
330 of coordination is achieved. In detail, TIFT provides joint-space walls that resist movement patterns that  
331 are inconsistent with the targeted shoulder-elbow inter-joint coordination pattern. Time independence is  
332 added to promote voluntary motion from the user without constraining the patient's arm to a fixed, rigid  
333 trajectory. Similarly, Crocher et al. (2010) proposed a controller which allows to impose velocity-based  
334 coordination through viscous force-field without constraining end-point motion. Specifically, the controller  
335 does not impose any trajectory, but it reacts user-applied forces by generating joint torques that restrict  
336 the motion when a certain velocity-based inter-joint coordination is not obtained. The same approach was  
337 used to perturb the human natural inter-joint coordination in healthy subjects Proietti et al. (2017). Results  
338 showed that the controller did not directly constrain end-effector movements, but it applied inter-joint  
339 velocity-dependent perturbing force fields distributed at the joint-level that disturbed the users' natural  
340 upper-limb coordination strategy.

341 Instead, besides the existence or not of a pre-defined desired trajectory, Kim and Deshpande (2015)  
342 presented a control strategy for the shoulder mechanism of an upper-body exoskeleton to assist in achieving  
343 coordinated motion at the shoulder complex. The idea is to introduce a coupling torque according to an  
344 impedance-based control law that adjusts the shoulder scapulohumeral rhythm configuration. The reference  
345 position for the shoulder elevation is computed according to an experimentally obtained quadratic law that  
346 correlates the shoulder elevation angle to the humerothoracic arm elevation. Such a relationship can be  
347 included and actuated both during free-space motion and along with exercise trajectories. In the first case,  
348 the controller implements a reactive action that corrects undesired postures with inter-joint coordination  
349 torques (Kim and Deshpande, 2017). The user can explore the range of motion using all the exoskeleton  
350 joints, and the corrective torques are applied only at certain joints to maintain the desired coupling. In the  
351 latter case, a proper inverse-kinematics algorithm includes inter-joint coordination constraints within the  
352 optimization problem. The algorithm exploits the kinematic redundancy of the robot (e.g., through the  
353 swivel angle) to reconfigure the exoskeleton according to the scapulohumeral rhythm and computes the  
354 desired joint trajectories (Dalla Gasperina et al., 2020).

355

#### 356 2.2.4 Assistance adaptation

357 However, to optimize the outcome of motor learning and to avoid the "slacking" effect, the assistance  
358 should be tailored to each stroke patient throughout the movements and over the rehabilitation treatment.  
359 Namely, the slacking behavior of the human motor control regards the patient that, trying to optimize  
360 the effort to accomplish a task, may learn to provide only the strictly sufficient amount of force needed  
361 to complete the task and it takes advantage of the exoskeleton assistance, which performs most of the  
362 physical effort (Marchal-Crespo and Reinkensmeyer, 2009). To avoid such a phenomena, the assistance  
363 should be supplied only when the subject is not able to actively complete the task and tailored to recovery  
364 stage. Different approaches for assistance adaptation have been explored in literature. They mainly involve  
365 trial-by-trial adaptation to modulate the robot assistance according to some user-specific performance  
366 metrics. For example, adapting control parameters is a key aspect of patient-cooperative strategies, by  
367 which the assistance can be automatically tailored to the participant's performances and needs. The goal is  
368 to keep the users engaged and actively participating to the treatment, by providing the minimum assistance  
369 level to fulfill the task and, at the same time, by promoting the maximum achievable patient muscular effort  
370 (Proietti et al., 2016). Adaptive assistance strategies are also referenced as assisted-as-needed strategies  
371 and are usually governed trial-by-trial through the following general adaptation control law:

$$u_i = fu_{i-1} + gE_i \quad (1)$$

372 where  $u_i$  is the assistance (or control parameter) that is adapted over time,  $E_i$  is a performance error or  
373 metric that can denote the capability of the participant to initiate the movement, to follow a desired path,  
374 or to reach a target, and  $i$  indicates the  $i^{th}$  trial.  $f$  is a forgetting factor ( $0 < f < 1$ ), included to avoid  
375 slacking and to promote continuous involvement of the participant and  $g$  is the gain that determines the  
376 reaction timing of the adaptation control law. Including the forgetting term is a key feature to challenge the  
377 participant, even if performance errors are low. Indeed, if we consider removing the forgetting term (i.e.,  
378  $f = 1$ ), the control parameters can saturate to the configuration that optimizes the performances, without  
379 taking into account the participant effort and engagement. According to the previously described taxonomy,  
380 adaptation can occur at both feedback and feedforward assistance loops. In the first case, robot stiffness  
381 and corrective force-fields are tuned according to the participants' abilities and effort. For instance, Krebs  
382 et al. (2003) first proposed a performance-based control algorithm, which tunes the corrective assistance  
383 according to speed, time, or EMG signals. Similarly, the correction can be tuned trial-by-trial according to  
384 error-based kinematic performance metrics (Proietti et al., 2015; Pérez-Ibarra et al., 2019). For example,  
385 the adaptation control law can rely on terms related to the difference between the measured trajectory and  
386 the one desired to fulfill the task, the normalized distance from a specific target, or indexes that indicate the  
387 accuracy in drawing a geometric shape (Stroppa et al., 2017b, 2018).

388 Alternatively, the adaptation can be applied to the feedforward assistance, as presented by Wolbrecht et al.  
389 (2008). The authors implemented an *assist-as-needed* controller that adapts the feedforward assistance,  
390 which is computed using radial basis functions and learned on subject's abilities. They added an error-based  
391 learning factor, which iteratively adapts the feedforward contribution, and a force decay, which reduces the  
392 support when the subject is able to perform the movement correctly.

### 393 2.3 Active modalities

394 Active modalities, also known as "transparent" modalities, are characterized by a "human-active/robot-  
395 passive" behavior. The robot does not provide assistance, nor resistance to the movement, and the subject  
396 is allowed to perform movements without perceiving the robot effort. Active modalities can be beneficial  
397 as they enable the exoskeleton to become a measurement device (Nordin et al., 2014). Recent studies

398 demonstrated that kinematic data can bring meaningful information to clinical assessment in post-stroke  
399 rehabilitation (Bigoni et al., 2016). De Oliveira et al. (2021) demonstrated that exoskeleton joint angle data  
400 are accurate measurements of arm and shoulder kinematics. However, when the robots are operated in  
401 active mode for assessment purposes, transparency is a fundamental feature. If the robot provides non-zero  
402 torque biases while the wearer is being evaluated, it generates undesired resistances during the upper-limb  
403 motion of subjects and it can consequently influence the performance and consequently the assessment  
404 (Proietti et al., 2016). When the robot is operated in active mode, the range of motion of each joint can be  
405 tuned and limited by control to avoid that the wearer overcomes physiological limits. Usually, range of  
406 motion boundaries are implemented through virtual walls, which can be implemented through repulsive  
407 virtual spring-damper systems.

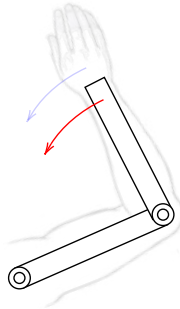
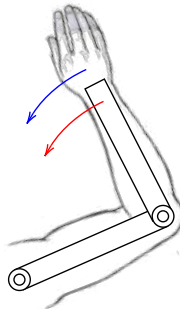
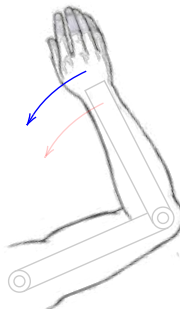
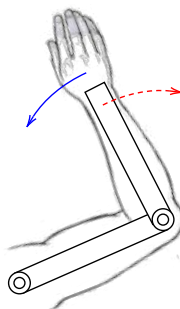
### 408 2.3.1 Tunneling strategies

409 As we previously described, corrective strategies usually provide assistance to help the subject follow the  
410 desired trajectory both along longitudinal and orthogonal directions. Conversely, the so-called tunneling  
411 strategies usually permit free movements, and they provide correction only when boundaries conditions  
412 are met. The concept is to create a virtual cylindrical channel at the end-effector that permits free active  
413 movements along the longitudinal direction, but restricts movements in radial directions by applying  
414 restoring forces to the end-effector position, if the user exits the virtual channel. In order words, tunneling  
415 strategies permit active free movement and bound the task-space or joint-space workspace with software  
416 virtual walls and boundaries. Since these strategies do not assist the movement along the trajectory main  
417 direction, as stated by Proietti et al. (2016), the concept is linked to time-independence of the task references.  
418 In particular, in such modalities, there are not trajectory profile references that relate position, velocity,  
419 and time. Instead, the controller is fed with a time-independent three-dimensional desired path. Guidali  
420 et al. (2011) implemented a tunneling strategy by subdividing the task in multiple sub-movements, and  
421 creating force-fields channels to correct the hand position within each sub-movement. Then, after the user  
422 had reached a way-point, a trajectory generator algorithm updates the trajectory for the next sub-movement.  
423 Similarly, Wu et al. (2018a) implemented a three-dimensional channel based on three concentric channels.  
424 The inner channel permits active free movements, the central one assists the user to reach the inner  
425 channel, while the outer channel restricts movement directed out of the virtual tunnel. In some works, a  
426 timeout-triggered assistance, also known as *back-wall*, is added to help the users to complete the task when  
427 they get stuck and they are not able to actively initiate or finish the movement. The *back-wall* is usually  
428 implemented through a pushing force along the longitudinal direction of the channel (Proietti et al., 2016).  
429 If such timeout-triggered assistance is present, tunneling strategies can be become assistive as well. Thus,  
430 the taxonomy can be confusing and it can be difficult to distinguish purely tunneling strategies, with or  
431 without *back-wall*, from active-assistive modalities.

### 432 2.4 Resistive modalities

433 Historically, rehabilitation robots were designed to assist the patient during the initial phases after stroke,  
434 i.e., when the patient is severely impaired and needs substantial assistance to complete functional tasks.  
435 Then, when the patient has (hopefully) relearned most of the lost motor functionalities but still has to gain  
436 some muscular tone, conventional therapy proposes gym-like body-weight exercises. Resistive modalities  
437 have been recently introduced as a rehabilitation solution for the latest stages of the motor recovery  
438 process to engage the patients during their progression through robot-mediated exercises. In fact, robots  
439 can provide an aquatic therapy-like environment that allows user-driven free movements with or without  
440 viscous resistance (Kong et al., 2010). Usually, resistive modalities do not follow trajectory references.  
441 Still, they permit the user to actively explore the workspace, and the exoskeleton resists user's movement  
442 through virtual viscous force-fields, which are usually inversely proportional to the movement velocity

443 (Song et al., 2014). Finally, we could include in this category also other challenging strategies based on  
444 error-augmentation methods since they indirectly resist the motion by repressing the voluntary movement or  
445 by emphasizing kinematics errors. Error-augmentation consists of algorithms that, through repulsive forces,  
446 amplify movement errors rather than decrease them (Patton et al., 2006). Indeed, as previously mentioned,  
447 motor learning has underlined that kinematic errors are fundamental neural signals to improve motor  
448 adaptation (Emken et al., 2007a). A similar approach involves instead the implementation of task-space  
449 force fields that push the user's arm away from equilibrium points or comfortable positions to enhance  
450 workspace exploration (Wright et al., 2015, 2018). Resistive and challenging modalities have been broadly  
451 investigated in gait and locomotion analysis. However, few studies have been performed in upper-limb  
452 functional rehabilitation (Abdollahi et al., 2014; Israely and Carmeli, 2016).

High-level modalities	Passive	Active-assistive	Active	Resistive
<b>Features</b>	The robot performs the task without accounting for subject's effort. The robot corrects trajectory errors.	The robot and the subject perform the task cooperatively. The robot can provide weight counterbalance or trajectory-based corrective assistance.	The subject actively performs the task. The robot does not provide assistance nor resistance to the subject. No time-dependent trajectory is present.	The subject actively performs the task. The robot resists to the movement by providing opposing forces.
<b>Human-robot interaction</b>				
<b>Rationale</b>	Prevents soft tissue stiffening. Passive mobilization generates somatosensory stimulation Passive-triggered strategies, Teach-and-replay strategies, Passive-mirrored strategies.	Preserves subject motivation and self-esteem. Subject's involvement promotes motor learning. Purely corrective and weight counterbalance assistance, Inter-joint coordination assistance, Adaptive assistance.	The robot is a measurement device. Permits ROM exploration and do not limit subject's voluntary free movements. Tunneling or trajectory-constrained strategies.	Promotes subject's involvement and potentiate muscular strength. Viscous-field and error-augmentation strategies.
<b>Variants</b>				

**Table 2.** High-level training modalities for upper-limb robot-mediated rehabilitation. Classification refers to subject's status at interaction. Red arrows represent exoskeleton assistance (solid) or resistance (dashed). Blue arrows indicate user voluntary effort, if present.

### 3 LOW-LEVEL ROBOT-ASSISTED CONTROL STRATEGIES

453 To guarantee a good collaboration of subject and exoskeleton during physical human-robot interaction,  
454 the robot should display a wide range of haptic mechanical impedance, which should span from high-  
455 compliance (low-resistance) to high-stiffness behaviors. While achieving rigid control can be considered  
456 trivial, promoting the so-called compliant motion, i.e., the robotic device should behave transparently to  
457 voluntary human activity, can be challenging. Furthermore, its performances are strongly related to the  
458 mechanical design of the actuation unit and thus they depend on the specific hardware implementation.  
459 Namely, compliant control refers to the capability of the robotic system to generate movement and,  
460 simultaneously, to undergo movement if external forces are applied. On the one side, the robot drives the  
461 motion of the limb and corrects for trajectory errors. On the other side, the user applies forces/torques to the  
462 robot, which should permit deviations from a defined equilibrium point without suppressing the voluntary  
463 activity. Since compliant motion doesn't limit in any way any intention of movement of the interacting user,  
464 it guarantees one of the most fundamental features for efficient motor recovery and demonstrated to be a  
465 fundamental, yet challenging, feature in rehabilitation robotics. To make the processes mentioned above  
466 interact smoothly, each of them should be aware of the other's behavior. While the human, thanks to its  
467 somatosensory and visual systems, can directly feel and monitor the behavior of the robot, both in terms of  
468 interaction forces and perceived movements, the robotic device needs an adequate sensors network to detect  
469 the involvement and the intention of movement coming from the user. Indeed, exoskeleton developers  
470 can follow different approaches to detect the user's intention of movement, which deeply depend on the  
471 implemented hardware.

472 Recently, Calanca et al. (2016) published a survey that presented the state of the art of compliant control  
473 algorithms according to the available sensor networks and control schemes. The authors analyzed solutions  
474 from traditional robotics, usually involving stiff joints, to more recent approaches that combine soft joints  
475 with advanced control schemes. Indeed, the concept of compliant motion refers to the capability of a system  
476 to shape the dynamical relation between motion and torque/forces, instead of independently controlling the  
477 joint motion or the joint torques of the robot. Thus, to promote compliant interaction between the human  
478 and the robot, along trajectories or in free motion, several low-level control strategies have been proposed  
479 (Miao et al., 2018). Most of the compliant controllers, instead of relying on high-gains corrective position  
480 control, implement nested control loops that are usually characterized by an inner high-accuracy loop,  
481 which guarantees fast response of the robotic system, and an outer "flexible" loop, which includes the  
482 human contribution and implements the interaction control. Such approaches mainly rely on two control  
483 schemes: Impedance control (force/torque based control) and its dual admittance control (position based  
484 control) Ott et al. (2010); Schumacher et al. (2019). However, as we previously introduced, the perceived  
485 compliance can be implemented either through compliant controllers, or through mechanical compliance,  
486 for example by using soft joints instead of stiff joints (Calanca et al., 2016, 2017; Schumacher et al., 2019).  
487 Thus, in this review, we include and discuss position control of soft joints as it can itself promote compliant  
488 interaction control.

#### 489 3.1 Impedance control

490 Among all, impedance control is one of the most common approaches, and it has been demonstrated to  
491 be a very efficient solution for neurorehabilitation (Marchal-Crespo and Reinkensmeyer, 2009; Mehdi and  
492 Boubaker, 2012). It implements dynamic control that shapes the desired mechanical impedance through  
493 human-robot interaction: a torque/force output is generated from a position input. In this section, we will

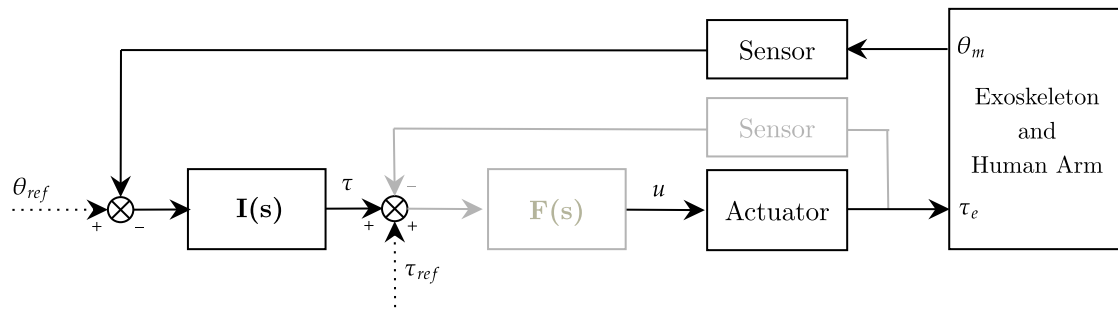


**Figure 3.** Impedance control scheme in the joint-space. Implicit (black) and explicit (black and gray).  $I(s)$  is the impedance controller,  $F(s)$  is the force controller (only explicit).  $\theta_{ref}$  and  $\tau_{ref}$  represent respectively reference angular position and torque, while  $u$  refers to the motor current control signal.

494 firstly describe the main features of impedance control applied to a joint of the robot (i.e., in the joint-space),  
 495 then we will explain its applicability in the Cartesian-space.

496 Impedance control was first introduced by Hogan (1985), and it is also referred to as force-based position  
 497 control or equilibrium point control. Indeed, differently from traditional position control, this approach  
 498 does not aim at precisely tracking trajectories, but it proposes a trade-off between interaction forces and  
 499 deviation from the reference motion. To promote this behavior, impedance control is characterized by a  
 500 nested loop architecture. An inner torque-feedback loop implements the transparent behavior and promotes  
 501 the mechanical compliance (i.e., it "softens" the control). An outer position-feedback loop corrects for  
 502 trajectory tracking errors by applying forces or torques aimed at the completion of the task (i.e., it "stiffens"  
 503 the control). Two different variants of the impedance control can be identified. When the actuation unit  
 504 is inherently back-drivable, the torque control can be implemented through an open-loop control loop  
 505 (i.e., implicit impedance). In the other cases, a loadcell or an elastic element is exploited in series as a  
 506 feedback signal for the closed-loop torque control loop (i.e., explicit impedance) (Khalil and Dombre,  
 507 2002). Explicit impedance control improves force sensitivity, but can jeopardize the coupled stability of the  
 508 human-robot system. In fact, high torque-loop control gains can cause stability issues when in contact with  
 509 hard surfaces (Focchi et al., 2016; Calanca et al., 2016), thus there exists a trade-off between torque fidelity  
 510 tracking and stability of the impedance controller. The impedance control schemes (implicit and explicit)  
 511 can be implemented in the joint-space as shown in Figure 3.

512 The reference or equilibrium joint position is  $\theta_{ref}$ , while the actual position  $\theta_m$  is usually measured by  
 513 motor encoders. The torque control signal  $\tau$  is usually computed as:

$$\tau = I(s)(\theta_{ref} - \theta_m) + \tau_{ref} \quad (2)$$

514 where  $I(s)$  is the mechanical impedance model, usually multiplied by the trajectory tracking error, and  
 515  $\tau_{ref}$  represents the torque reference, often used to compensate for gravity and friction torques. The actuator  
 516 block represents the actuator dynamics and converts the control signal  $u$  to the desired output. If the explicit  
 517 impedance control scheme is exploited,  $F(s)$  represents the inner torque control loop, which is in charge  
 518 of making sure that the measured torque output ( $\tau_e$ ) tracks its reference ( $\tau + \tau_{ref}$ ). The  $F(s)$  estimates the  
 519 target torque of the actuator ( $u$ ), usually through a Proportional–Integrative–Derivative (PID) controller.  
 520 The impedance filter  $I(s)$  is generally described by a  $n^{th}$  polynomial system that varies according to the  
 521 order of the virtualized mechanical impedance system. Impedance control of  $0^{th}$  order, also referenced as

522 pure stiffness control (Trigili et al., 2020), is formally equivalent to a proportional (P) position controller,  
 523 where the gain represents the desired mechanical stiffness  $K_s$  (Equation 3).

$$I(s) = K_s \quad (3)$$

524 If a 1<sup>st</sup> order impedance is implemented, the velocity error, namely  $\dot{\theta}_{ref} - \dot{\theta}_m$ , is multiplied by a target  
 525 damping coefficient  $K_d$ , which is usually aimed at reducing jerky oscillations and dissipating spring energy.  
 526 The 1<sup>st</sup> order impedance control formally corresponds to a proportional-derivative (PD) position controller  
 527 (Equation 4).

$$I(s) = K_s + sK_d \quad (4)$$

528 This is one of the most common implementations in rehabilitation robotics as the virtual stiffness, by  
 529 means of the virtual spring constant  $K_s$ , pulls the joint link towards its reference (i.e., the spring corrects  
 530 for deviations from the joint trajectory), while the virtual damper  $K - d$  dampens oscillations and stabilizes  
 531 the movement. However, in most cases, since the desired velocity  $\dot{\theta}_{ref}$  is not accessible, the desired velocity  
 532 can be neglected and set to zero, and the damping coefficient only multiplies the measured velocity. In this  
 533 way, the damping term is related to the absolute velocity instead of the error velocity, and the controller  
 534 always provides resistance to the motion, regardless if the user is correctly following or not the desired  
 535 trajectory (Kim and Deshpande, 2017). In time domain, the control law becomes:

$$\tau = K_s(\theta_{ref} - \theta_m) + K_d(\dot{\theta}_m) + \tau_{ref} \quad (5)$$

536 Finally, impedance control of 2<sup>nd</sup> order allows to shape also the desired mass/inertia  $K_i$  of the system.  
 537 When dealing with rehabilitation robots, usually the desired mechanical inertia is the one of the human  
 538 arm, thus the second order term can be neglected. The control law becomes as in Eq. 6, which corresponds  
 539 to a proportional-integral-derivative (PID) velocity controller.

$$I(s) = K_s + sK_d + s^2K_i \quad (6)$$

540 Higher order implementations are possible, and the desired impedance can be set to be of arbitrary order.  
 541 However, if higher orders are concerned, the impedance control parameters would become physically  
 542 meaningless, and the computation of high order derivatives can introduce noise to the acceleration signals.  
 543 In this view, first order impedance control is usually preferred.

544 In rehabilitation robotics, many exoskeletons are controlled in the task-space through Cartesian-space  
 545 impedance controllers (Frisoli et al., 2009; Nef et al., 2009a). This approach is preferred over joint-space  
 546 impedance control since it favors functional tasks, and it does not require inverse-kinematics algorithms  
 547 during trajectory generation. The Cartesian-space impedance control scheme is implemented by virtualizing  
 548 a mechanical impedance in the task-space instead of at the joint level, as shown in Figure 4. While in  
 549 joint-space the spring-damper system is a rotational system  $n$ -dimensional ( $n$  represents the number  
 550 of active degrees-of-freedom of the robot), in Cartesian-space, the mechanical impedance is linear and  
 551 three-dimensional. In fact, the corrective action is provided by three-dimensional forces, usually referred  
 552 to as corrective force-fields. Consequently, in order to permit the robot to generate such assistance, there  
 553 is the need to convert 3-dimensional task-space forces to  $n$ -dimensional joint-space torques. Generally,  
 554 the transposed Jacobian matrix is exploited to compute such conversion. The Cartesian-space impedance

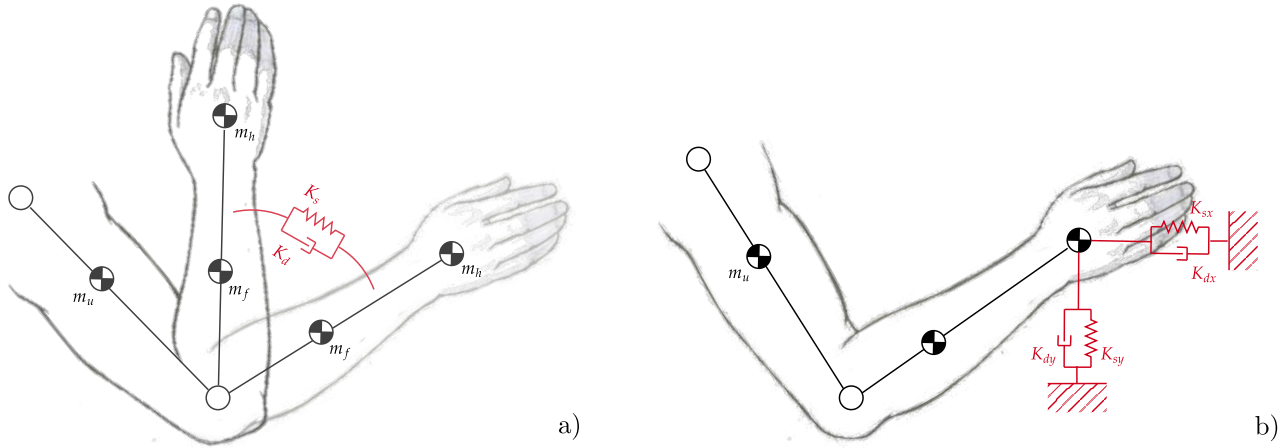


**Figure 4.** (a) First order impedance model applied at the elbow joint in the joint-space. (b) First order impedance model applied at the elbow joint in the Cartesian-space.

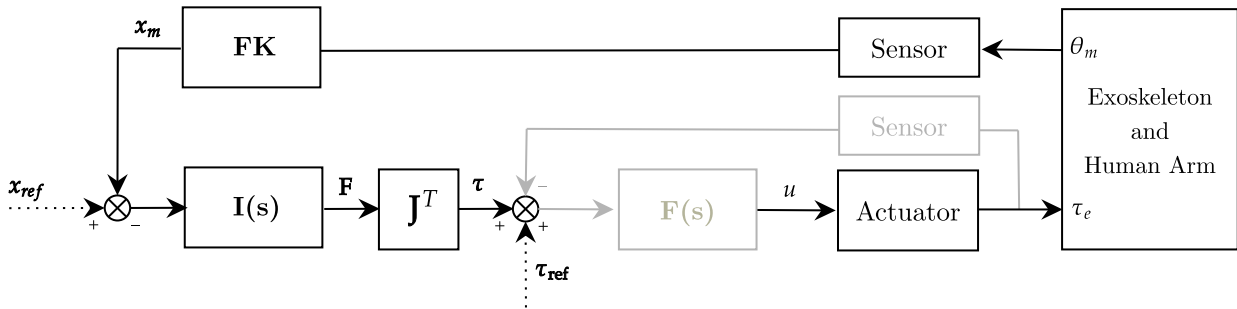


**Figure 5.** Impedance control scheme in the Cartesian-space. Implicit (black) and explicit (black and gray).  $I(s)$  is the impedance controller,  $F(s)$  is the force controller (only explicit).  $FK$  represents the forward kinematics model of the exoskeleton, and  $J^T$  corresponds to the transposed Jacobian matrix.  $\theta_{ref}$  and  $\tau_{ref}$  represent respectively reference angular position and torque, while  $u$  refers to the motor current control signal.

555 control scheme is considered a centralized control approach, since it exploits the robot configuration  
 556 (usually through forward kinematics) to compute the desired torques at each joint, as shown in Figure 5.

557 In detail, considering a 1<sup>st</sup> order mechanical impedance on the  $x$  Cartesian-direction, the force-fields are  
 558 computed as:

$$F_x = K_s(x_{des} - x_m) - K_d(\dot{x}_{des} - \dot{x}_m) \quad (7)$$

559 where  $K_s$  and  $K_d$  are the desired linear spring and damper, respectively, and  $x_m$  is the measured position  
 560 of the end-effector, computed through the forward kinematics model of the exoskeleton.

561 In neurorehabilitation, Cartesian-space impedance controllers can be used to implement tunneling  
 562 strategies. They permit to discriminate robot assistance along the tangential and orthogonal directions of the  
 563 end-effector reference motion. Thus, the robot can assist along the axial tunnel direction and correct along  
 564 the radial direction. Cartesian impedance strategies also intrinsically allow time-independent relationships  
 565 among the exoskeleton joints, which is crucial to enable the user to exhibit voluntary movements. In

566 fact, besides the robot configuration, the ultimate goal is to control the pose of the user's hand through  
 567 spring-damper behavior to follow the desired path. However, this strategy (i.e., Cartesian impedance  
 568 control) does not control or correct compensatory movements or non-coordination among joints. Therefore,  
 569 it is more prone to maladaptive plasticity mechanisms. For example, Zhang et al. (2020) presented a  
 570 novel assisted-as-needed controller that, through a task-space impedance controller, assists the position  
 571 of the hand of the user to follow a virtual tunnel. Stiffness fields are created to push the end-effector  
 572 to the center of the tunnel and guide it along the tunnel if the user is not fast enough. Furthermore, the  
 573 proposed controller can be adjusted through five adjustable parameters to implement different robot-aided  
 574 rehabilitation training such as passive, active-assistive, active, and resistive training.

### 575 3.2 Admittance control

576 Admittance control is the dual approach to impedance control, and it is generally used as a method to  
 577 promote physical human-robot interaction with stiff, non-backdrivable actuators (Keemink et al., 2018).  
 578 By definition, admittance control actuates motion (usually position or velocity) through a force/torque  
 579 feedback, and it is also generally known as position-based impedance control or impedance control with  
 580 force feedback (Ott et al., 2010). The control scheme involves a nested loop architecture, where the inner  
 581 loop controls the position (or velocity) of the joint, and the outer torque loop computes the motion setpoint  
 582 according to the desired human-robot interaction, as shown in Figure 6.

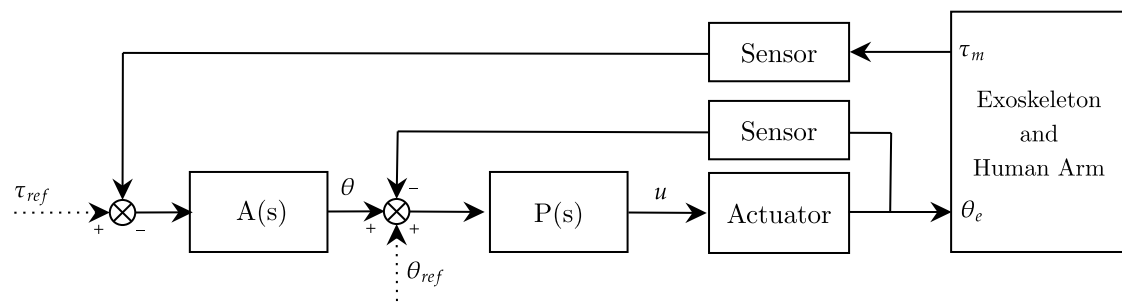


**Figure 6.** Admittance control scheme in the joint-space.  $A(s)$  is the admittance controller,  $P(s)$  is the position controller.  $\theta_{ref}$  and  $\tau_{ref}$  represent respectively reference angular position and torque, while  $u$  refers to the motor current control signal.

583 In admittance control, the inner loop "stiffens" the joint, and the outer loop "softens" the human-robot  
 584 interaction behavior (Calanca et al., 2016). Generally, robot weight compensation is not needed since the  
 585 robot is position controlled. However, in some works, weight compensation is provided in feedforward at  
 586 the inner position control loop ( $P(s)$ ) to improve trajectory tracking Bai et al. (2017). The main advantage  
 587 of using admittance control in rehabilitation robotics is that it does not require intrinsic back-drivability  
 588 of the actuation unit: the inner motion control loop intrinsically compensates and rejects stiction and  
 589 dynamic friction. In other words, the outer force loop computes the reference motion that produces a  
 590 virtual backdrivability of the joint (Calanca et al., 2016). When dealing with impedance control, achieving  
 591 high-fidelity torque control is critical to render a wide variety of mechanical impedance (Z-width), i.e.,  
 592 impedance control requires both high-stiffness gains for good trajectory tracking and low-stiffness gains  
 593 to promote compliant behavior and its accuracy depends on the capability of the system to deliver high-  
 594 quality torques. Contrarily, admittance control can exploit the standard features of industrial robots for the  
 595 implementation of the inner motion loop that can suppress undesired disturbances such as system dynamics

596 and friction, without the need for model-based compensation (Schumacher et al., 2019). The main limitation  
 597 arises when low-impedance behavior is desired, and high-admittance gains could lead to instability issues.  
 598 Similar to impedance control, different orders of the admittance filter can be selected. Still, the computation  
 599 of the reference motion profile in the time-domain may require numerical integration to solve the motion  
 600 differential equations. In this review, we will consider the admittance model as the relationship between  
 601 force and position (Ott et al., 2010; Schumacher et al., 2019). In other studies, such as in Calanca et al.  
 602 (2016), authors described the admittance model as a force-velocity relationship. The admittance model  
 603 of zero-order is usually referred to as compliance control, and it is formally complementary to stiffness  
 604 control, by means of the inverse of the desired stiffness  $K_d$ . The desired zero-order admittance is computed  
 605 as:

$$\mathbf{A}(s) = 1/K_d = K_d^{-1} \quad (8)$$

606 The 1<sup>st</sup> order admittance or accommodation control is one of the most common implementations in  
 607 rehabilitation since it is suitable for slow motion (Keemink et al., 2018). The motion is derived from the  
 608 force/torque feedback as follows:

$$\mathbf{A}(s) = 1/(K_d + sD_d) = (K_d + sD_d)^{-1} \quad (9)$$

609 where  $D_d$  represents the desired impedance damping (or viscous friction).

610 For example, Zhuang et al. (2019) proposed a first-order admittance model, characterized by a virtual  
 611 spring-damper interaction system, to control an ankle rehabilitation exoskeleton promoting compliant  
 612 behavior. By neglecting the zero-order desired stiffness  $K_d$ , the impedance model becomes a pure anti-  
 613 damping velocity-driven admittance controller, which is generally the simplest way to promote transparent  
 614 behavior at the joint level.

615 Finally, the second-order admittance model also permits to shape the desired mass/inertia  $M_d$  of the  
 616 virtualized dynamic system. The admittance equation is shown in (10).

$$\mathbf{A}(s) = \frac{1}{(K_d + sD_d + s^2M_d)} = (K_d + sD_d + s^2M_d)^{-1} \quad (10)$$

617 The desired stiffness can be removed, and the controller becomes a mass-damper virtualized system, as in  
 618 Chia et al. (2020).

619 When coming to rehabilitation exercises, the position-controlled trajectories are generally computed  
 620 as the sum of the desired joint profiles, namely  $\theta_{ref}$ , and the angle  $\theta$  that is in turn obtained from the  
 621 admittance model and the interaction forces. In this way, the robot follows the desired movement but  
 622 permits deviation according to the user's voluntary activity. The reference torque  $\tau_{ref}$  is normally used to  
 623 filter out gravity effects and static disturbances from the torque/force measurements  $\tau_m$ , but it can also  
 624 be tuned to include additional external force-fields to the desired physical human-robot interaction. For  
 625 upper-limb robots, admittance control in the joint-space (i.e., with torque feedback at the joints level) has  
 626 not been explored yet, since it requires precise mathematical models for gravity compensation. Instead,  
 627 6-DOFs force/torque sensors at the interaction ports of the robot are more often exploited to detect the  
 628 interaction effort with the user. With this approach, there is no need for gravity compensation of the  
 629 robot (which is position-controlled), and the force feedback does not need additional filtering for gravity

630 effects. Of course, since the force/torque sensors usually detect interaction in the three-dimensional space,  
 631 a conversion to joint-space motion is needed to feed the inner control loops (that operate at each joint of  
 632 the robot). If task-space sensors are used, the conversion can be implemented both for the desired position  
 633 or for the measured feedback. The admittance control scheme for task-space sensors is shown in Figure 7.

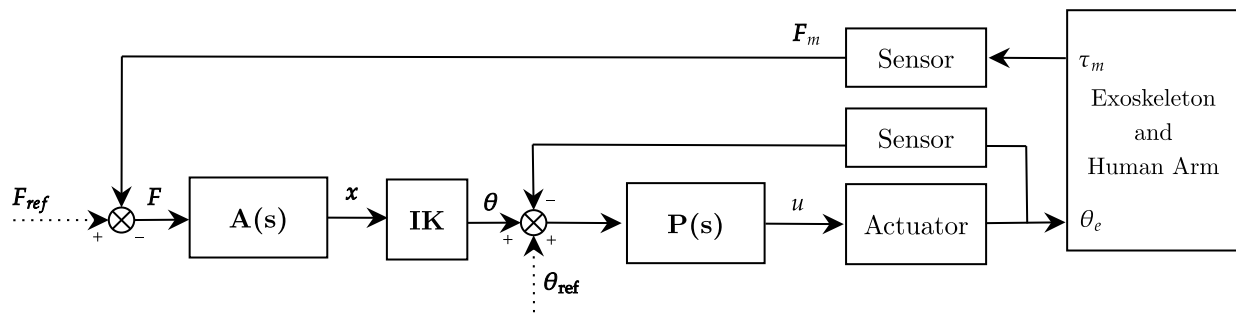


**Figure 7.** Admittance control scheme in the task-space.  $A(s)$  is the task-space admittance controller,  $P(s)$  is the joint-space position controller.  $IK$  corresponds to the inverse-kinematics algorithm.  $\theta_{ref}$  and  $\tau_{ref}$  represent respectively reference angular position and torque, while  $u$  refers to the motor current control signal.

634 With respect to the task/joint space conversion, Wu et al. (2018b) developed a patient-active admittance  
 635 controlled exoskeleton for upper-limb neurorehabilitation. Interaction forces with the user are acquired  
 636 with force/torque sensors at the end-effector. The differential desired forces are then fed to a second-order  
 637 admittance filter that computes the desired differential trajectory in task space. Finally, an inverse kinematics  
 638 algorithm computes the desired trajectories in the joint-space. Alternatively, Bai et al. (2017) implemented  
 639 a second-order admittance control scheme with an upper-limb exoskeleton. The forces are measured at the  
 640 arm cuffs through force-sensing contact sensors. The sensors measure the human-robot interaction forces,  
 641 which are analyzed by a "force model controller" that computes the desired interaction torque for each  
 642 joint. Finally, the admittance filter is applied to compute the motion profiles in the joint-space.

643 As previously mentioned, in admittance control, the intrinsic back-drivability of the exoskeleton joint  
 644 is not needed. In fact, the robot is position-controlled by the inner loop, which does not guarantee to be  
 645 intrinsically transparent to user effort, and external signals are used to detect the intention of movement  
 646 towards a certain direction. Many different approaches are available to detect user-driven movements. The  
 647 most common approach relies on direct measurement of interaction effort through force/torque sensors at  
 648 the interface ports of the robot that are usually at the upper arm and forearm cuffs (Kim and Deshpande,  
 649 2017; Wu et al., 2018a,b) (Section 4.2). Alternatively, human voluntary effort can be estimated by means  
 650 of EMG-based sensing (Zhuang et al., 2019), or with force-sensing resistors (FSR) (Bai et al., 2017).

#### 4 HARDWARE-LEVEL IMPLEMENTATION OF COMPLIANT CONTROL

651 When dealing with rehabilitation exoskeletons, most platforms rely on electric motors provided with high-  
 652 ratio gearboxes to increase the ability to deliver motor torque. However, they are inherently inefficient and  
 653 they introduce non-linear stiction, static and viscous friction, and reflected inertia, which can compromise  
 654 back-drivability (Schumacher et al., 2019). Consequently, in most cases the perceived compliance cannot be  
 655 guaranteed by the mechanical back-drivability of the geared drive itself, and users would need to overcome  
 656 large torques to initiate voluntary movements (Nef and Lum, 2009). In this review, we focus on electrically

657 powered exoskeletons and we describe three global approaches to promote compliant behavior with geared  
658 drives, i.e., to permit the user exert torque onto the robot joint, according to the desired low-level control  
659 strategies.

#### 660 **4.1 Model-based compensation**

661 When dealing with implicit impedance controlled exoskeletons, by which the robot is not provided with  
662 additional torque sensors, residual frictional torques need to be compensated by software. A common  
663 practice to improve back-drivability of high-ratio gearboxes is to implement friction compensation models  
664 (Weiss et al., 2012; Nef and Lum, 2009). In this way, a zero-torque controller could achieve good  
665 transparency with low residual resistive torques. Usually, friction is modeled with a kinetic friction term  
666 (Coulomb and viscous velocity-dependent) and a breakway friction term, which relates to the stiction  
667 phenomena (Armstrong, 1988). The friction compensation is mainly regarded as positive velocity-based  
668 feedforward control (Just et al., 2016). Still, the breakaway friction usually cannot be compensated for  
669 since the sign of the compensation term depends on the direction of the desired movement, which is not  
670 always defined a priori (Nef and Lum, 2009).

#### 671 **4.2 Interaction force/torque sensing**

672 Researchers are recently providing their rehabilitation robots and exoskeletons with torque/force sensors,  
673 which directly measure the interaction force between the human and the robot (Villani and De Schutter,  
674 2008), namely achieving active compliant control. For impedance control approaches, direct torque sensing  
675 permits to implement torque control loops with explicit feedback to reject friction disturbances and to  
676 reduce residual resistive torques (Boaventura et al., 2012, 2013). Overall, this approach leads to better  
677 torque-tracking performances and improves back-drivability. However, Focchi et al. (2016) demonstrated  
678 that high-gain tuning of the torque closed-loop can jeopardize the stability of the robot when touching hard  
679 surfaces. Thus, there exists a compromise between low undesired interaction forces and control robustness  
680 (Vallery et al., 2008). Torque sensing can also be fed in at the outer loop, such as in admittance control. In  
681 this case, the robot is not compliant because of the inner loop, but the effort sensing is used to update the  
682 desired trajectory of the inner loop. While torque sensing in impedance control is usually performed in the  
683 joint-space, with admittance control, the loadcell is usually installed at the end-effector, through a handle,  
684 or at the interaction ports, through the arm cuffs that are usually at the upper arm and at the forearm levels  
685 (Kim and Deshpande, 2017; Wu et al., 2018a; Kumar et al., 2019). While in most cases the interaction  
686 forces are measured with loadcell-based sensors, sometimes force sensing resistors (FSR) are installed  
687 inside arm cuffs (Bai et al., 2017).

#### 688 **4.3 Mechanical compliance (SEA)**

689 While the first two approaches are usually implemented with rigid joints, the perceived compliance can  
690 also be implemented by adding mechanical compliance, for example by using soft joints. In fact, compliant  
691 control can be also achieved by voluntarily introducing elastic elements (i.e., springs) in series to general  
692 purpose electric actuators, namely series elastic actuators (SEA) (Vallery et al., 2008). Several research  
693 groups that develop upper-limb exoskeletons are now relying on SEAs (Crea et al., 2016; Chen et al., 2019;  
694 Wu et al., 2019) since they are inherently safe, they permit robust force control and they are efficient in  
695 periodic tasks (Calanca et al., 2016). Also, if additional mechanical compliance is added to the actuation  
696 chain, there is no need for a intrinsic backdrivable geared actuator. However, SEAs, due to the mechanical  
697 compliance, result in limited force and position control bandwidth, and can lead to instability issues when  
698 trying to achieve high-impedance behavior. Namely, the achievable displayed stiffness of the joint cannot  
699 be higher than the physical spring stiffness of the SEA, if passivity is desired (Vallery et al., 2008; Calanca  
700 et al., 2017).

701 The mechanical compliance can potentially simplify the control strategy of the exoskeleton. For example,  
702 in Wu et al. (2019) Trigli et al. (2020), compliant control was achieved by position-controlling a SEAs unit.  
703 Indeed, there is no need to strictly apply compliant control strategies, since the compliance is intrinsically  
704 provided by the physical stiffness. Nevertheless, in most cases, a combination of impedance/admittance  
705 control of SEA is used to promote variable impedance behavior Calanca et al. (2016). In some other cases,  
706 if the spring stiffness is high enough, the SEA does not provide a perceivable mechanical compliance, but  
707 the spring is used only to indirectly compute the joint torque output by measuring its displacement and to  
708 dampen high frequency oscillations (Kim and Deshpande, 2017).

709 Overall, if impedance control strategies are desired, there is the need for good back-drivability of the  
710 joint to promote compliant interaction control. Instead, admittance control typically does not require  
711 back-drivable joints, and high transmission ratios are preferred to achieve precise position control, but  
712 force/torque sensing is mandatory to detect the intention of movement of the user. Finally, if SEA-based  
713 joint are designed, compliance is intrinsically promoted, and torque sensing can be achieved with indirect  
714 measurements based on the elastic element deformation.

## 5 AVAILABLE EXOSKELETON PROTOTYPES

715 This section presents and compares some control solutions for arm rehabilitation exoskeleton prototypes  
716 available in the literature. The presented list is non-comprehensive, but works were selected to describe and  
717 demonstrate how different approaches could promote similar high-level rehabilitation modalities. Indeed,  
718 we focused on works that describe how the three levels of implementation have been combined to obtain a  
719 given high-level training behavior. For each solution, we explain its functioning at the three levels of the  
720 proposed classification, and we report the key findings of each approach.

721

### 5.1 The AAU exoskeleton

723 The exoskeleton described in Bai et al. (2017); Christensen and Bai (2018) is an upper-limb device  
724 provided with three actuated DOFs and one passive DoF, developed at the Aalborg University (AAU). The  
725 proposed solution addresses the problem related to the design of the shoulder mechanism, allowing the  
726 exoskeleton to match the complex motion of the human shoulder joint. The proposed kinematics relies  
727 on a spherical mechanism consisting of two revolute joints connected through a double parallelogram  
728 linkage. The exoskeleton is equipped with force sensing resistors (FSR) sensors (capable of detecting  
729 physical pressure) to measure the interaction between the user and the exoskeleton. Such measurements  
730 are elaborated by a *force model controller* module capable of detecting the direction of the applied  
731 interaction forces. Based on the magnitude and direction of the applied forces, the admittance controller  
732 has been implemented to provide the subject with the capabilities to operate the exoskeleton based on the  
733 applied interaction. Such admittance controller defines the reference velocity for the inner PI trajectory  
734 tracking controller with gravity compensation capabilities, allowing to operate the exoskeleton. Preliminary  
735 experimental results have shown the performance of the proposed design.

### 5.2 The ALEx exoskeleton

737 The Arm Light Exoskeleton (ALEx) is a bimanual robotic device specifically designed for robot-supported  
738 rehabilitation of stroke patients. ALEx is a cable-driven, mechanically compliant exoskeleton operated  
739 by four actuated and sensorized DOFs (shoulder and elbow) and two passive DOFs (wrist). The robot is  
740 equipped with brushless motors located remotely to the exoskeleton joints. The use of compliant cable-  
741 based transmission reduces weight and inertia of the system, and the mechanical compliance, introduced  
742 by cables, permits to achieve robust force control (Stroppa et al., 2017a). In its first version, ALEx allows

743 to perform movements in three different modalities: i) *robot-passive*, namely human-active modality  
744 according to our classification (i.e., the participant moves the arm in the workspace and the robot follows  
745 the motion), ii) *robot-active*, namely human-passive modality according to our classification (i.e., the  
746 robot guides the participant's arm during the movement), and iii) *assisted-as-needed*, or passive-triggered  
747 modality, by which the robot guides the motion only if a timeout-based trigger is reached (Pirondini  
748 et al., 2016). At the low-level, the exoskeleton can be operated in *force mode*, which provides desired  
749 forces at the end-point, or in *compliant position mode*, which relies on independent position control of  
750 the robot compliant joints. For all modalities, the low-level force controller is computed as the sum of  
751 several feedforward contributions, including gravity compensation of the moving robotics links, friction  
752 compensation of transmission mechanisms, and inertia compensation of moving parts. In a recent study,  
753 Stroppa et al. (2017b) presented an adaptive assistance controller based on a Cartesian-space impedance  
754 control scheme. The impedance law is based on a mass-spring-damper dynamic system that corrects joint  
755 trajectories in the task-space. Finally, the assist-as-needed paradigm is implemented according to an online  
756 performance evaluation of the subject's motor skills.

### 757 **5.3 The ARAMIS exoskeleton**

758 The ARAMIS exoskeleton is a bi-manual exoskeleton for upper-limb neurorehabilitation after stroke.  
759 The robotic platform includes two fully motorized 6-DOFs symmetric exoskeletons (Pignolo et al., 2012).  
760 The robot can operate in different modalities that involve the use of both the unaffected and the paretic arm  
761 (Pignolo et al., 2016). In *synchronous mode*, which can be addressed as master-replica mode, the robot  
762 supports the impaired limb of the subject and replicates the sample movements performed by the other  
763 arm in real-time. In *asynchronous mode*, instead, the contralateral exoskeleton arm first records a sample  
764 movement, then the robot actively supports the paretic arm along the mirrored task. Such trajectories can  
765 be recorded either by the patient's unaffected limb or by the therapist's guidance (Dolce et al., 2009). The  
766 ARAMIS exoskeleton can also operate in *weight counterbalance mode*: the robot compensates for the  
767 arm weight during movements replicating those executed by the contralateral side (Pignolo et al., 2016).  
768 Each joint of the robot is actuated by DC brushed motors coupled with high transmission ratio gearboxes.  
769 To enhance the backdrivability of the system, the authors developed an integrated joint that relies on a  
770 SEA-based design (Colizzi et al., 2009). Series springs are connected at the output shaft of the actuator,  
771 and a secondary encoder measures the spring displacement. In this way, the controller can detect whether  
772 the patient initiates the movement and the exoskeleton follows the user-driven action.

### 773 **5.4 The ARMin exoskeleton(s)**

774 The ARMin exoskeleton is an upper-limb rehabilitation robot developed at the Sensory-Motor Systems  
775 Lab, ETH Zurich. The exoskeletal system has been conceived to promote task-oriented, repetitive, and  
776 intensive arm training in patients with upper extremities paralysis (Nef et al., 2009a). In its early versions,  
777 ARMin is actuated with six DOFs. Four of them are controlled by implicit impedance control laws, while  
778 two are operated in admittance mode (Oldewurtel et al., 2007). The two DOFs controlled in admittance  
779 promote shoulder elevation and translation movements and rely on force/torque measurement of a 6-axis  
780 sensor at the shoulder joint. The robot is embedded with model-based friction and inverse dynamics  
781 compensation to improve transparency and minimize interaction forces with the human limb. In Nef  
782 et al. (2007), the ARMin II can operate in two different high-level modalities, according to the patients'  
783 recovery stage. In *passive mobilization mode*, first, the therapist moves the patient's arm together with  
784 the robot on the desired trajectory. In this phase, the robot's gravity and friction are compensated so that  
785 the therapist feels only the forces and torques necessary to move the human arm. Then, an algorithm  
786 extracts relevant way-points during the movement and computes a minimum jerk trajectory to be followed  
787 by the passive mobilization therapy with adjustable velocity. The authors also implemented a ball game

788 based on an *assistive mode*: the subject has to catch a virtual ball rolling down an inclined virtual table.  
789 Through a Cartesian-space impedance control law, the robot supports the user by driving their hand along  
790 the horizontal plane with gradient force-fields assistance that pushes the patient's arm towards the ball  
791 position. Guidali et al. (2011) presented a further development of ARMin III. The authors built a virtual  
792 tunnel around the task-space reference trajectory allowing the user to move freely within the tunnel while  
793 guided at the tunnel walls. Furthermore, the exercise could be triggered by the patients' voluntary activity  
794 when the user effort overcomes a certain threshold, and the movement is directed to the next task. In a  
795 recent study, the researchers improved the ARMin IV exoskeleton's transparency through a velocity-based  
796 disturbance observer. They compared it to the more traditional friction, gravity, and inertia feedforward  
797 compensation (Just et al., 2018). Finally, three distinct methods for arm weight compensation using the  
798 ARMin exoskeleton were proposed and analyzed (Just et al., 2020). All three methods are based on  
799 anthropometric arm models and are generalizable for use in different robotic devices and various subjects.

## 800 **5.5 The CleverARM exoskeleton**

801 The CLEVERarm is an 8-DOFs lightweight and ergonomic upper-limb rehabilitation exoskeleton  
802 for upper-limb impairment developed at the Texas A&M University, capable of producing diverse and  
803 perceptually rich training scenarios Soltani-Zarrin et al. (2018); Zeiaee et al. (2019). The robot supports  
804 the motion of the shoulder girdle, glenohumeral joint, elbow, and wrist. Six degrees of freedom of the  
805 exoskeleton are active, and the two degrees of freedom supporting the wrist motion are passive. The  
806 CLEVERarm joints employ electric motors coupled with harmonic drive actuators, and the mechatronic  
807 system is provided with force/torque sensors at the two interaction points with the arm to enable achieving  
808 back-drivability of the exoskeleton. The control scheme relies on an impedance-based controller employed  
809 to track rehabilitation exercises implemented in the game environment. The *path generator* computes  
810 human-like motions that support the scapulohumeral rhythm Soltani-Zarrin et al. (2017). Additionally, the  
811 controller is provided with a gravitational model of the robot to cancel the weight of the exoskeleton, and a  
812 friction compensation method, achieved through an admittance-based controller. Finally, the interaction  
813 forces measured by the F/T sensors are used to compute the desired velocity of the interaction ports to  
814 improve the back-drivability of the exoskeleton. Then, the desired angular velocities are computed through  
815 the system Jacobian and are fed as references to the impedance-based controller Soltani-Zarrin et al. (2018).

## 816 **5.6 The EXO-UL8 exoskeleton**

817 The EXO-UL8 is a dual-arm exoskeleton that covers all the main movements of a human's upper limb.  
818 The robot supports the motion of the shoulder, elbow, and wrist through seven non-backdrivable joints,  
819 and an additional joint operates the handgrip Shen et al. (2019). In a previous version, the EXO-UL7 was  
820 actuated through cable-driven actuation mechanisms. Now, the EXO-UL8 is operated by electric motors  
821 coupled with harmonic drives. A set of four force/torque sensors are placed at the physical interaction  
822 points between the user and the exoskeletal system. The robot relies on an admittance controller that  
823 allows the exoskeleton to behave transparently to user-driven movements. Precisely, torques applied by the  
824 human to the exoskeleton joints are estimated from the F/T sensors, then, through an admittance model,  
825 reference trajectories are generated and operated by the inner low-level PID control loops. Friction and  
826 gravity compensation is added as feedforward terms to the low-level controller Shen et al. (2019). The  
827 core concept of the EXO-UL8 controller is to generate motion in response to human-applied forces to  
828 improve backdrivability and reduce the user-perceived weight of the robot. On top of this, the system can  
829 be operated to follow pre-defined trajectories for rehabilitation exercises. Since the authors developed a  
830 dual-arm symmetric system, they also enabled mirroring training modes based on bilateral teleoperation  
831 between unimpaired and impaired arms. Additionally, Shen et al. (2018) proposed an asymmetric bilateral  
832 training using an interactive virtual reality environment.

### 833 5.7 The FELXO-Arm1 exoskeleton

834 The FELXO-Arm1 system is an upper-limb exoskeleton for neurorehabilitation. It supports shoulder and  
835 elbow movements through 5-DOFs aligned with human upper-limb joints to match natural physiological  
836 synergies. Lin et al. (2021) presented a control strategy for customized robot-assisted passive rehabilitation.  
837 The method aims to coordinate shoulder and elbow movements during the early stage of the rehabilitation  
838 treatment. The authors proposed a teaching training strategy by which the therapist provides desired  
839 trajectories by driving the impaired limb of the patient in the workspace. The trajectory is then adjusted in  
840 position, velocity, and acceleration to promote movement smoothness and continuity. Then, the movement  
841 is repeated over time with high intensity. The exoskeleton joints are controlled by a proportional differential-  
842 based trajectory tracking controller based on an implicit impedance control law. The inverse dynamic  
843 model of the system is computed according to the Lagrange method, and the generated torques are included  
844 as a feedforward torque controller. The FELXO-Arm1 exoskeleton is powered by BLDC electric motors  
845 coupled with harmonic drive gearboxes. A friction compensation algorithm rejects residual dynamic and  
846 breakthrough friction at each joint to improve transparency and compliant behavior. Torque sensors measure  
847 human-robot interactive torques at shoulder and elbow joints to identify the movement intention of the  
848 patient.

### 849 5.8 The Harmony exoskeleton

850 Kim and Deshpande (2017) developed an upper-body bi-manual exoskeleton for post-stroke rehabilitation  
851 aimed at providing natural coordination at the shoulder complex. The robotic exoskeleton consists of seven  
852 degrees-of-freedom (DOFs) for each arm: five DOFs are used to assist the shoulder and the scapulohumeral  
853 rhythm, one DOFs assists the elbow flexion/extension, and one operates the wrist pronation/supination.  
854 The authors developed a baseline controller that implements active modalities with joint-coordination  
855 constraints (Kim and Deshpande, 2015; Dalla Gasperina et al., 2020). The *baseline controller* promotes  
856 joint transparency, corrects for non-coordinated scapulohumeral rhythm through an impedance control law  
857 (spring-damper corrective assistance), and compensates for the robot weight through positive feedback that  
858 is computed inverse dynamics recursive algorithm (weight counterbalance assistance). The exoskeleton is  
859 actuated with SEAs, which are used to compute an indirect measure of torque by measuring the deformation  
860 of the elastic element. The exoskeleton can also be operated with an explicit joint-space impedance control  
861 scheme to follow desired trajectories De Oliveira et al. (2019), and it can promote different high-level  
862 modalities ranging from *assistive* to *resistive* modalities. Finally, the mechatronic system is also provided  
863 with force/torque 6-axis sensors at the interaction upper arm and forearm cuffs, and it can be operated to  
864 display a desired stiffness in the Cartesian space as well (Kim and Deshpande, 2017).

### 865 5.9 The L-EXOS exoskeleton

866 Frisoli et al. (2005) developed a force-feedback cable-driven light exoskeleton (L-EXOS) for  
867 rehabilitation. The L-EXOS robot operates four active DOFs: three DOFs assist the shoulder ball-socket  
868 joint, and one DOF is devoted to the elbow movements. In Frisoli et al. (2009), the robot is controlled  
869 in *assistive mode*, and the robot assists the motion only when the subject is not able to complete the  
870 rehabilitation exercise. In detail, the controller discriminates longitudinal and orthogonal direction with  
871 respect to the reference trajectory and promotes a virtual tunnel that follows the task-space desired  
872 trajectory. From a lower-level perspective, two concurrent task-space impedance controllers act along  
873 the tangential and orthogonal directions of the trajectory and compute the desired restoring forces at the  
874 end-effector. The transposed Jacobian matrix is used to convert task-space forces to joint-space torques,  
875 that are actuated accordingly. The dynamic model of the exoskeleton is derived from CAD models and  
876 the weight compensation of the device is implemented with a feedforward torque contribution. The robot

877 is actuated with permanent magnet torque actuators, that do provide intrinsic backdrivability. Also, the  
878 design of the exoskeleton was conducted following a set of guidelines to improve the transparency of the  
879 device, such as choosing high power density actuators, low transmission ratios, and low backlash gearboxes.  
880 Furthermore, motors were placed remotely with respect to the actuation joint using tendon transmissions to  
881 minimize the perceived inertia due to the motors' weight.

## 882 **5.10 The NEUROExos Shoulder-Elbow Module (NESM) exoskeleton**

883 The NEUROExos Shoulder-Elbow Module (NESM) is an exoskeleton for upper-limb neurorehabilitation  
884 and spasticity treatment. It actuates 4-DOFs, namely 3-DOFs at the shoulder and 1-DOF at the elbow (Crea  
885 et al., 2016). The exoskeleton joints are composed of high-torque SEA units, which permit high-fidelity  
886 torque control and introduce mechanical compliance to accommodate users' voluntary movements. Torque-  
887 sensing is achieved in joint-space by indirect measurement on the series-spring displacement. The robot  
888 can operate in various training modalities, such as passive mobilization, active-assisted, active-resisted,  
889 and active-disturbed training modes. In order to adapt the robot assistance to a wide range of patients'  
890 residual movements, the exoskeleton is provided with two control macro-modalities: *robot-in-charge* and  
891 *patient-in-charge* programs (Trigili et al., 2020). In the *robot-in-charge* approach, the robot passively  
892 mobilizes the human arm along pre-defined joint trajectories. The joints are position-controlled through a  
893 standard PID scheme, and the intrinsic serial elasticity provides additional compliance to accommodate  
894 spasticity and uncomfortable positions. Joint trajectories are computed through an inverse-kinematics  
895 algorithm by selecting maximum joint or hand velocities. Instead, in *patient-in-charge* mode, each joint of  
896 the exoskeleton is torque-controlled. In particular, the feedback torque is derived from the series-spring  
897 elongation, and a PID scheme tracks the desired torque. In this macro-mode, the robot promotes compliant  
898 control, behaves transparently to user-initiated movements, assists and resists the user's movements at  
899 each joint according to the desired training modality. The authors also present some additional sub-modes.  
900 In transparent mode, the robot tracks the null-torque and compensates for its weight. In impedance  
901 control mode, a dual (convergent and divergent) explicit impedance control scheme assists (or disturbs)  
902 the motion along the desired joint trajectories. Finally, three variants of muscle strength training modes  
903 are implemented to training specific muscular groups in a resistive-like manner. In all patient-in-charge  
904 sub-modalities, a gravity compensation algorithm iteratively computes the gravity torque of each joint  
905 due to the robot weight. Then, the gravity torque is fed as a torque feedforward contribution to the central  
906 controller (Crea et al., 2017).

## 907 **5.11 The NTUH-II exoskeleton**

908 The NTUH-II exoskeleton is an upper-limb device for robotic rehabilitation for shoulder-impaired  
909 patients (Lin et al., 2014). Such exoskeleton is provided with 8 DOFs, being able to reproduce most of  
910 the shoulder movements, such as shoulder flexion/extension, horizontal abduction/adduction, and rotation.  
911 The exoskeleton has been provided with the following control schema (Chia et al., 2020). A Kalman  
912 filter has been designed in order to estimate the human torques. An admittance model is then used to  
913 access the active motion of the human (therefore, making it possible to estimate the user's intention of  
914 motion). On top of that, a velocity field is designed in order to provide active assistance to the subject  
915 in interaction with the exoskeleton. Finally, an integration method is proposed in order to combine the  
916 admittance model output with the velocity field output, providing the reference signal to the exoskeleton  
917 controller, computing the torques to be applied by the motors. The main contribution that has been given  
918 by the proposed control approach is related to the velocity field: it provides a method for the generation of  
919 time-independent assistance based on the given rehabilitation task. In order to implement the proposed  
920 velocity field, the considered rehabilitation task has to be parameterized. After that, the path is encoded  
921 using the velocity field to make the assistance time-independent. The adopted velocity field is capable

922 to assist the subject to execute the target task along the tangential direction of the reference trajectory  
923 while compensating for deviations along the normal directions. Experimental results have demonstrated  
924 the capabilities of the proposed approach to assist the subject during the rehabilitation task execution.

### 925 **5.12 The Pneu-WREX exoskeleton**

926 The Pneu-WREX exoskeleton is an upper-limb device for robot-aided movement training following  
927 stroke (Wolbrecht et al., 2008). The Pneu-WREX exoskeleton is provided with 4 pneumatically actuated  
928 DOFs. The following three main characteristics have been implemented in the proposed device: mechanical  
929 compliance, the ability to assist patients in completing desired movements, and the ability to provide only  
930 the minimum necessary assistance. In order to provide active assistance to the subject, the exoskeleton  
931 is controlled exploiting two control loops: an inner controller based on a standard model-based, adaptive  
932 control approach in order to learn the patient's abilities and assist in completing movements while remaining  
933 compliant, and an outer *assistance-as-needed* controller defining a force term to the adaptive control law.  
934 Such an outer controller decays the force output from the robot when errors in task execution are small,  
935 while it increases the assistance to the user when errors in task execution are bigger. The proposed controller  
936 has been demonstrated to be successful in experimental tests executed with people who have suffered a  
937 stroke.

### 938 **5.13 The RECUPERA exoskeleton**

939 Kumar et al. (2019) recently presented a lightweight dual-arm rehabilitation robot called RECUPERA  
940 exoskeleton. The exoskeleton offers a high level of modularity. It can be used as a wheelchair-mounted  
941 system or as a full-body system for therapist-guided and self-training for neurorehabilitation of the upper  
942 body. The wheelchair-mounted version features 5-DOFs for each arm, while the full-body operates 30  
943 DOFs. The RECUPERA exoskeleton implements three different rehabilitation training modalities, namely  
944 *gravity compensation*, *teach-and-replay*, and *master-slave* therapy. In *gravity compensation* mode, the  
945 robot compensates for its weight through an inverse dynamic model of the exoskeleton. This mode can also  
946 include the compensation of the human arms dynamic model, and it is conceived as the baseline controller  
947 of the robot. The *teach-and-replay* mode consists of two phases. First, the robot is operated in gravity  
948 compensation mode, and the therapist performs a trajectory that is recorded by the system. Afterward, the  
949 robot detects a trigger from the user (or from the therapist) and passively performs the recorded movement.  
950 Finally, the *master-slave* mode consists of a mirroring strategy by which the paretic arm follows and mimics  
951 the trajectory performed with the healthy arm operated in gravity compensation mode. The RECUPERA  
952 exoskeleton is powered by high-torque BLDC actuators coupled with low-backlash gearboxes to increase  
953 torque output at the joint axis. The joints are controlled with cascaded position, velocity, and current  
954 control loops, while torque control is achieved through motor current measurements. The exoskeleton is  
955 also provided with 6-DOFs force/torque sensors to detect human-robot interaction at the three interfaces:  
956 hand, forearm, and upper arm interaction ports.

957 As shown in Table 3, different "low-level" control strategies can be used to promote the same "high-level"  
958 modalities, and there is not a unique relationship between the three layers. The majority of upper-limb  
959 exoskeletons are conceived upon the foundation of compliant control, by which the user should have the  
960 lead when performing the rehabilitation task. The robot should always follow the user's intention and  
961 apply corrective actions only when the residual muscular forces are insufficient to fulfill the action. Among  
962 low-level compliant control strategies, impedance control is the most used since it outperforms admittance  
963 control strategies when low-impedance behavior (i.e., transparent free motion) is desired. Furthermore, we  
964 underline the importance of achieving high-quality compliant control, either through high-fidelity torque  
965 control in conjunction with impedance control strategies or through torque/force-sensing combined with

966 admittance control. Indeed, many researchers rely on force feedback, which can be obtained either via  
967 SEA-based indirect measurements or torsional/linear loadcell-based direct measurements. Many studies  
968 demonstrated that torque feedback could improve the performances of compliant control over model-based  
969 compensation methods. However, the introduction of additional sensors can drastically increase prototype  
970 costs. Series elastic actuators are gaining increasing interest since they provide inexpensive, accurate torque  
971 sensing at the joint and introduce mechanical compliance to promote compliant motion. However, with  
972 SEAs, it is impossible to achieve higher stiffness than the elastic element, reducing the robot performances  
973 when high-impedance (rigid) interaction is required.

Exoskeleton	Supported joints	DOFs	Bimanual	High-level	Low-level	Actuation	Sensing	References
AAU	S,E	3	no	none	Admittance (with gravity compensation)	brushless motor coupled with harmonic drive gearbox	task-space force sensing resistors (FSK)	Bai et al. (2017)
ALEX	S,E	4x2	yes	Passive (passive-triggered), Active-assistive (adaptive assistance) and Active modalities	Position control of compliant joints, Task-space force control, Cartesian impedance control (with friction, gravity and inertia compensation)	brushless DC motor coupled with mechanically compliant cable transmission	no	Pirondini et al. (2016); Stroppa et al. (2017b)
ARAMIS	S,E,W	6x2	yes	Passive (mirroring), Active-assistive (counterbalance)	Position control of SEA-based joints	SEA-based brushed DC motor coupled with gearbox	joint-space (SEA-based indirect)	Colizzi et al. (2009); Pignolo et al. (2012, 2016)
ARMIn	S,E,W	6	no	Passive, Active-assistive (corrective, tunneling)	Joint-space and task-space implicit impedance control (with friction and dynamics compensation)	brushed DC motor, coupled with harmonic drive gearbox	task-space (6-axis FT sensor, only ARMIn II and III)	Nef et al. (2009b); Guidali et al. (2011); Just et al. (2020)
CLEVERarm	S,E,W	6	no	Passive, and Active-assistive.	joint-space impedance control (with friction and gravity compensation) and admittance-based control for back-drivability	electric DC motor coupled with harmonic drive gearboxes	task-space (6-axis FT sensors)	Soltani-Zarinn et al. (2018)
EXO-UL8	S,E,W	7	yes	Passive and Active-assistive (symmetric and asymmetric mirroring), Active (transparent) modalities.	task-space admittance control (with friction and gravity compensation) and inner joint-space position control	electric DC motor, coupled with harmonic drive gearboxes	task-space (6-axis FT sensors)	Shen et al. (2018, 2019)
FELXO-ArmI	S,E	5	no	Passive (teach-and-replay), Active-assistive.	joint-space implicit impedance control	brushless DC motor coupled with harmonic drive gearboxes	joint-space (direct)	Lin et al. (2021)
Harmony	S,E,W	7x2	yes	Active-assistive (corrective and counterbalance), Active (inter-joint coordination) and Resistive modalities	Explicit impedance control (with friction and dynamics compensation)	SEA-based brushless DC motor	joint-space (SEA-based indirect), task-space (6-axis FT sensors)	Kim and Deshpande (2017)
L-Exos	S,E	4	no	Active-assistive (corrective), Active (tunneling).	Task-space implicit impedance control (with friction and gravity compensation)	quasi-backdrivable magnet torque motor	no	Frisoli et al. (2005, 2009)
NESM	S,E	4	no	Passive, Active-assistive, Resistive (viscous-field and error-augmentation)	Position control of SEA-based joints, joint-space explicit impedance control	SEA-based brushless DC motor coupled with harmonic drive gearboxes and custom springs	joint-space (SEA-based indirect)	Crea et al. (2016); Trigili et al. (2020)
NTUH-II	S,E,W	8	no	Active-assistive (velocity-field control)	Admittance control	brushless DC motor coupled with gearbox	task-space (6-axis FT sensors at wrist and upper arm)	Lin et al. (2014); Chia et al. (2020)
Pneu-WREX	S,E	4	no	Active-assistive (assistance-as-needed)	Model-based adaptive impedance control	pneumatic actuation	no	Wolbrecht et al. (2008)
RECUPERA	S,E,W	5x2	yes	Passive (mirroring), Active-assistive (counterbalance).	Position, velocity, current control	brushless DC motor coupled with low-backlash gearboxes	task-space (6-axis FT sensors)	Kumar et al. (2019)

**Table 3.** Comparison of available control strategies at high-level, low-level and hardware-level for upper-limb neurorehabilitation exoskeletons. S: shoulder, E: elbow, W: wrist.

## 6 CONCLUSION

974 Control advancements for upper-limb exoskeletons for rehabilitation are spreading rapidly, and the literature  
975 continuously presents new prototypes and control approaches. Since we noticed that state-of-the-art reviews  
976 on controls for rehabilitation robots generally focus their attention on training modalities and human-robot  
977 interaction, our study was intended to propose a multi-disciplinary taxonomy of patient-cooperative control  
978 strategies for rehabilitation upper-limb exoskeletons that could help researchers develop complex and  
979 advanced systems. Our classification is based on a three-level scheme: on i) *high-level training modalities*,  
980 ii) *low-level control strategies*, and iii) *hardware-level implementation*. Overall, we report that most  
981 high-level modalities are based on assistive approaches, by which the robot partially supports the user  
982 during the motion. In turn, most exoskeletons support human movements in three ways. On one side, they  
983 provide corrective assistance, either through impedance-based strategies or via tunneling methods that  
984 guide the user to stay within a specific virtual path. Alternatively, weight counterbalance, also known as  
985 anti-gravity support, can be implemented to compensate for gravity due to the user's arm. Finally, inter-joint  
986 coordination is involved whether the aim is to induce physiological coordination based on position, torque,  
987 or velocity-based synergies.  
988

989 In Figure 8, we report a summary of the aspects we investigated in this work, intending to help robotics  
990 researchers bridge the gap between desired rehabilitation outcomes and robotic implementation. The  
991 reader can interpret the scheme following both bottom-up and top-down paradigms: i) the exoskeleton  
992 control design process can both start from the available hardware (actuator, sensors, etc.) to define the  
993 implementable control strategies for the desired behavior, or ii) researchers can identify the hardware  
994 requirements from the selected high-level training modalities.

995 In conclusion, this review presents an interdisciplinary vision on control solutions for upper-limb  
996 exoskeletons that suggest how different approaches can render physical human-robot interaction at different  
997 levels of implementation to promote the desired rehabilitation behavior. We noticed that most high-level  
998 training modalities are derived from motor learning concepts to improve the rehabilitation outcomes, and  
999 exoskeletons are usually programmed to mimic the therapist's actions during conventional treatment. We  
1000 suggest that to exploit robotic assistance to promote motor recovery, more neurological-inspired modalities  
1001 should be investigated to deepen the effects of robot-mediated therapy on neural plasticity and motor  
1002 relearning. Finally, further research is needed to evaluate which approach (at each level) is associated with  
1003 a more significant improvement of arm functions after stroke.

## CONFLICT OF INTEREST STATEMENT

1004 SDG, AP, FB and MG hold shares in AGADE Srl, Milano, Italy. The remaining authors declare that the  
1005 research was conducted in the absence of any commercial or financial relationships that could be construed  
1006 as a potential conflict of interest.

## FUNDING

1007 This work was partially supported by Regione Lombardia, Italy (Grant number: ARIA (formerly ARCA)  
1008 2018.132).

Hardware-level implementation		Low-level control strategies	
<b>Actuation hardware</b>	<b>Sensing hardware</b>	<b>Impedance (torque) control:</b>	
<b>Stiff joints:</b>	<b>Joint-space:</b>	- implicit vs explicit (only with joint torque sensors)	
- electric motors	- torsional loadcells	- joint-space vs task-space	
- brushed vs brushless	- SEA-based sensing	- SEA-based	
- gearbox	<b>Task-space:</b>	<b>Admittance (position) control</b> (only with force/torque sensors)	
<b>Soft joints:</b>	- 6-axis F/T sensors	<b>Position control</b> (only with soft joints)	
- SEA-based	- force interaction sensor	<b>Feedforward compensation:</b>	
- cable-driven	- FSR	- friction compensation	
	<b>No sensors</b>	- cable transmission compensation (only with cable-driven joints)	
		- gravity compensation	
		- inertia compensation	
<b>High-level training modalities</b>			
<b>Passive:</b>	<b>Active-assistive:</b>	<b>Active:</b>	<b>Resistive:</b>
- passive mobilization	- corrective assistance	- ROM boundaries	- viscous-field resistance
- passive triggered	- trajectory-based vs tunneling	- tunneling strategies	- error-augmentation
- teach-and-replay	- weight counterbalance assistance	- trajectory-constrained strategies	
- mirror training	- inter-joint coordination assistance		
	- adaptive assistance		

**Figure 8.** Summary of patient-cooperative control strategies for upper-limb rehabilitation exoskeletons at different levels of implementation: hardware-level actuation and sensing implementation, low-level control strategies, and high-level training modalities.

## REFERENCES

- 1009 Abdollahi, F., Case Lazzaro, E. D., Listenberger, M., Kenyon, R. V., Kovic, M., Bogey, R. A., et al. (2014).  
 1010 Error augmentation enhancing arm recovery in individuals with chronic stroke: A randomized crossover  
 1011 design. *Neurorehabilitation and Neural Repair* 28, 120–128. doi:10.1177/1545968313498649  
 1012 Ambrosini, E., Ferrante, S., Zajc, J., Bulgheroni, M., Baccinelli, W., D’Amico, E., et al. (2017). The  
 1013 combined action of a passive exoskeleton and an EMG-controlled neuroprosthesis for upper limb stroke  
 1014 rehabilitation: First results of the RETRAINER project. *IEEE International Conference on Rehabilitation  
 1015 Robotics*, 56–61doi:10.1109/ICORR.2017.8009221  
 1016 Ambrosini, E., Gasperini, G., Zajc, J., Immick, N., Augsten, A., Rossini, M., et al. (2021). A Robotic  
 1017 System with EMG-Triggered Functional Electrical Stimulation for Restoring Arm Functions in Stroke  
 1018 Survivors. *Neurorehabilitation and Neural Repair* 35, 334–345. doi:10.1177/1545968321997769  
 1019 Armstrong, B. (1988). Friction: experimental determination, modeling and compensation. In *Proceedings.  
 1020 1988 IEEE International Conference on Robotics and Automation* (IEEE Comput. Soc. Press), 1422–  
 1021 1427. doi:10.1109/ROBOT.1988.12266  
 1022 Bai, S., Christensen, S., and Islam, M. R. U. (2017). An upper-body exoskeleton with a novel shoulder  
 1023 mechanism for assistive applications. In *IEEE/ASME International Conference on Advanced Intelligent  
 1024 Mechatronics, AIM* (Institute of Electrical and Electronics Engineers Inc.), 1041–1046. doi:10.1109/  
 1025 AIM.2017.8014156  
 1026 Ballester, B. R., Maier, M., Duff, A., Cameirão, M., Bermúdez, S., Duarte, E., et al. (2019). A critical time  
 1027 window for recovery extends beyond one-year post-stroke. *Journal of Neurophysiology* 122, 350–357.

- 1028 doi:10.1152/jn.00762.2018
- 1029 Barsotti, M., Leonardis, D., Loconsole, C., Solazzi, M., Sotgiu, E., Procopio, C., et al. (2015). A full  
1030 upper limb robotic exoskeleton for reaching and grasping rehabilitation triggered by MI-BCI. In *2015*  
1031 *IEEE International Conference on Rehabilitation Robotics (ICORR)* (IEEE), vol. 2015-Septe, 49–54.  
1032 doi:10.1109/ICORR.2015.7281174
- 1033 Basteris, A., Nijenhuis, S. M., Stienen, A. H., Buurke, J. H., Prange, G. B., and Amirabdollahian, F.  
1034 (2014). Training modalities in robot-mediated upper limb rehabilitation in stroke: A framework for  
1035 classification based on a systematic review. *Journal of NeuroEngineering and Rehabilitation* 11, 1–15.  
1036 doi:10.1186/1743-0003-11-111
- 1037 Bastian, A. J. (2008). Understanding sensorimotor adaptation and learning for rehabilitation. *Current*  
1038 *Opinion in Neurology* 21, 628–633. doi:10.1097/WCO.0b013e328315a293
- 1039 Bernhardt, J., Hayward, K. S., Kwakkel, G., Ward, N. S., Wolf, S. L., Borschmann, K., et al. (2017).  
1040 Agreed definitions and a shared vision for new standards in stroke recovery research: The Stroke  
1041 Recovery and Rehabilitation Roundtable taskforce. *International Journal of Stroke* 12, 444–450.  
1042 doi:10.1177/1747493017711816
- 1043 Bertani, R., Melegari, C., De Cola, M. C., Bramanti, A., Bramanti, P., and Calabrò, R. S. (2017). Effects  
1044 of robot-assisted upper limb rehabilitation in stroke patients: a systematic review with meta-analysis.  
1045 *Neurological Sciences* 38, 1561–1569. doi:10.1007/s10072-017-2995-5
- 1046 Bigoni, M., Baudo, S., Cimolin, V., Cau, N., Galli, M., Pianta, L., et al. (2016). Does kinematics add  
1047 meaningful information to clinical assessment in post-stroke upper limb rehabilitation? A case report.  
1048 *Journal of Physical Therapy Science* 28, 2408–2413. doi:10.1589/jpts.28.2408
- 1049 Boaventura, T., Medrano-Cerda, G. A., Semini, C., Buchli, J., and Caldwell, D. G. (2013). Stability and  
1050 performance of the compliance controller of the quadruped robot HyQ. *IEEE International Conference*  
1051 *on Intelligent Robots and Systems*, 1458–1464doi:10.1109/IROS.2013.6696541
- 1052 Boaventura, T., Semini, C., Buchli, J., Frigerio, M., Focchi, M., and Caldwell, D. G. (2012). Dynamic  
1053 torque control of a hydraulic quadruped robot. *Proceedings - IEEE International Conference on Robotics*  
1054 *and Automation*, 1889–1894doi:10.1109/ICRA.2012.6224628
- 1055 Brackenridge, J., Bradnam, L. V., Lennon, S., Costi, J. J., and Hobbs, D. A. (2016). A review of  
1056 rehabilitation devices to promote upper limb function following stroke. *Neuroscience and Biomedical*  
1057 *Engineering* 4, 25–42. doi:10.2174/2213385204666160303220102
- 1058 Brauchle, D., Vukelić, M., Bauer, R., and Gharabaghi, A. (2015). Brain state-dependent robotic  
1059 reaching movement with a multi-joint arm exoskeleton: Combining brain-machine interfacing and  
1060 robotic rehabilitation. *Frontiers in Human Neuroscience* 9, 564. doi:10.3389/fnhum.2015.00564
- 1061 Brokaw, E. B., Holley, R. J., and Lum, P. S. (2013). Comparison of joint space and end point space robotic  
1062 training modalities for rehabilitation of interjoint coordination in individuals with moderate to severe  
1063 impairment from chronic stroke. *IEEE Transactions on Neural Systems and Rehabilitation Engineering*  
1064 21, 787–795. doi:10.1109/TNSRE.2013.2238251
- 1065 Calanca, A., Muradore, R., and Fiorini, P. (2016). A review of algorithms for compliant control of stiff  
1066 and fixed-compliance robots. *IEEE/ASME Transactions on Mechatronics* 21, 613–624. doi:10.1109/  
1067 TMECH.2015.2465849
- 1068 Calanca, A., Muradore, R., and Fiorini, P. (2017). Impedance control of series elastic actuators: Passivity  
1069 and acceleration-based control. *Mechatronics* 47, 37–48. doi:10.1016/j.mechatronics.2017.08.010
- 1070 Chang, J. J., Tung, W. L., Wu, W. L., Huang, M. H., and Su, F. C. (2007). Effects of Robot-Aided  
1071 Bilateral Force-Induced Isokinetic Arm Training Combined With Conventional Rehabilitation on Arm  
1072 Motor Function in Patients With Chronic Stroke. *Archives of Physical Medicine and Rehabilitation* 88,

- 1073 1332–1338. doi:10.1016/j.apmr.2007.07.016
- 1074 Chen, T., Casas, R., and Lum, P. S. (2019). An Elbow Exoskeleton for Upper Limb Rehabilitation with  
1075 Series Elastic Actuator and Cable-Driven Differential. *IEEE Transactions on Robotics* 35, 1464–1474.  
1076 doi:10.1109/TRO.2019.2930915
- 1077 Chia, E.-Y., Chen, Y.-L., Chien, T.-C., Chiang, M.-L., Fu, L.-C., Lai, J.-S., et al. (2020). Velocity  
1078 Field based Active-Assistive Control for Upper Limb Rehabilitation Exoskeleton Robot. In *2020*  
1079 *IEEE International Conference on Robotics and Automation (ICRA)* (IEEE), 1742–1748. doi:10.1109/  
1080 ICRA40945.2020.9196766
- 1081 Christensen, S. and Bai, S. (2018). Kinematic analysis and design of a novel shoulder exoskeleton using a  
1082 double parallelogram linkage. *Journal of Mechanisms and Robotics* 10. doi:10.1115/1.4040132
- 1083 Cieza, A., Causey, K., Kamenov, K., Hanson, S. W., Chatterji, S., and Vos, T. (2020). Global estimates of  
1084 the need for rehabilitation based on the Global Burden of Disease study 2019: a systematic analysis for  
1085 the Global Burden of Disease Study 2019. *The Lancet* 396, 2006–2017. doi:10.1016/S0140-6736(20)  
1086 32340-0
- 1087 Colizzi, L., Lidonnici, A., and Pignolo, L. (2009). The ARAMIS project: A concept robot and technical  
1088 design. *Journal of Rehabilitation Medicine* 41, 1011–101. doi:10.2340/16501977-0407
- 1089 Colombo, R., Pisano, F., Micera, S., Mazzone, A., Delconte, C., Chiara Carrozza, M., et al. (2005). Robotic  
1090 techniques for upper limb evaluation and rehabilitation of stroke patients. *IEEE Transactions on Neural*  
1091 *Systems and Rehabilitation Engineering* 13, 311–324. doi:10.1109/TNSRE.2005.848352
- 1092 Crea, S., Cempini, M., Moise, M., Baldoni, A., Trigili, E., Marconi, D., et al. (2016). A novel shoulder-  
1093 elbow exoskeleton with series elastic actuators. *Proceedings of the IEEE RAS and EMBS International*  
1094 *Conference on Biomedical Robotics and Biomechatronics* 2016-July, 1248–1253. doi:10.1109/BIOROB.  
1095 2016.7523802
- 1096 Crea, S., Cempini, M., Moisè, M., Baldoni, A., Trigili, E., Marconi, D., et al. (2017). Validation of  
1097 a gravity compensation algorithm for a shoulder-elbow exoskeleton for neurological rehabilitation.  
1098 In *Biosystems and Biorobotics* (Springer International Publishing), vol. 15. 495–499. doi:10.1007/  
1099 978-3-319-46669-9{-}82
- 1100 Crespo, L. M. and Reinkensmeyer, D. J. (2008). Effect of robotic guidance on motor learning of a timing  
1101 task. In *Proceedings of the 2nd Biennial IEEE/RAS-EMBS International Conference on Biomedical*  
1102 *Robotics and Biomechatronics, BioRob 2008*. 199–204. doi:10.1109/BIOROB.2008.4762796
- 1103 Crocher, V., Sahbani, A., and Morel, G. (2010). Imposing joint kinematic constraints with an upper limb  
1104 exoskeleton without constraining the end-point motion. *IEEE/RSJ 2010 International Conference on*  
1105 *Intelligent Robots and Systems, IROS 2010 - Conference Proceedings* , 5028–5033doi:10.1109/IROS.  
1106 2010.5650961
- 1107 Dalla Gasperina, S., Ghonasgi, K., De Oliveira, A. C., Gandolla, M., Pedrocchi, A., Deshpande, A.,  
1108 et al. (2020). A novel inverse kinematics method for upper-limb exoskeleton under joint coordination  
1109 constraints. In *IEEE International Conference on Intelligent Robots and Systems* (Institute of Electrical  
1110 and Electronics Engineers Inc.), 3404–3409. doi:10.1109/IROS45743.2020.9341686
- 1111 De Oliveira, A. C., Sulzer, J. S., and Deshpande, A. D. (2021). Assessment of Upper-Extremity Joint Angles  
1112 Using Harmony Exoskeleton. *IEEE Transactions on Neural Systems and Rehabilitation Engineering* 29,  
1113 916–925. doi:10.1109/TNSRE.2021.3074101
- 1114 De Oliveira, A. C., Warburton, K., Sulzer, J. S., and Deshpande, A. D. (2019). Effort estimation in  
1115 robot-aided training with a neural network. In *Proceedings - IEEE International Conference on Robotics*  
1116 *and Automation*. vol. 2019-May, 563–569. doi:10.1109/ICRA.2019.8794281

- 1117 Dipietro, L., Ferraro, M., Palazzolo, J. J., Krebs, H. I., Volpe, B. T., and Hogan, N. (2005). Customized  
1118 interactive robotic treatment for stroke: EMG-triggered therapy. *IEEE Transactions on Neural Systems  
1119 and Rehabilitation Engineering* 13, 325–334. doi:10.1109/TNSRE.2005.850423
- 1120 Dolce, G., Lucca, L. F., and Pignolo, L. (2009). Robot-assisted rehabilitation of the paretic upper limb:  
1121 Rationale of the ARAMIS project. *Journal of Rehabilitation Medicine* 41, 1007–1010. doi:10.2340/  
1122 16501977-0406
- 1123 Emken, J. L., Benitez, R., and Reinkensmeyer, D. J. (2007a). Human-robot cooperative movement training:  
1124 Learning a novel sensory motor transformation during walking with robotic assistance-as-needed.  
1125 *Journal of NeuroEngineering and Rehabilitation* 4, 1–16. doi:10.1186/1743-0003-4-8
- 1126 Emken, J. L., Benitez, R., Sideris, A., Bobrow, J. E., and Reinkensmeyer, D. J. (2007b). Motor adaptation  
1127 as a greedy optimization of error and effort. *Journal of Neurophysiology* 97, 3997–4006. doi:10.1152/jn.  
1128 01095.2006
- 1129 Focchi, M., Medrano-Cerda, G. A., Boaventura, T., Frigerio, M., Semini, C., Buchli, J., et al. (2016).  
1130 Robot impedance control and passivity analysis with inner torque and velocity feedback loops. *Control  
1131 Theory and Technology* 14, 97–112. doi:10.1007/s11768-016-5015-z
- 1132 Frisoli, A., Loconsole, C., Leonardis, D., Bannò, F., Barsotti, M., Chisari, C., et al. (2012). A new  
1133 gaze-BCI-driven control of an upper limb exoskeleton for rehabilitation in real-world tasks. *IEEE  
1134 Transactions on Systems, Man and Cybernetics Part C: Applications and Reviews* 42, 1169–1179.  
1135 doi:10.1109/TSMCC.2012.2226444
- 1136 Frisoli, A., Rocchi, F., Marcheschi, S., Dettori, A., Salsedo, F., and Bergamasco, M. (2005). A new  
1137 force-feedback arm exoskeleton for haptic interaction in virtual environments. In *Proceedings - 1st Joint  
1138 Eurohaptics Conference and Symposium on Haptic Interfaces for Virtual Environment and Teleoperator  
1139 Systems; World Haptics Conference, WHC 2005* (Institute of Electrical and Electronics Engineers Inc.),  
1140 195–201. doi:10.1109/WHC.2005.15
- 1141 Frisoli, A., Salsedo, F., Bergamasco, M., Rossi, B., and Carboncini, M. C. (2009). A force-feedback  
1142 exoskeleton for upper-limb rehabilitation in virtual reality. *Applied Bionics and Biomechanics* 6,  
1143 115–126. doi:10.1080/11762320902959250
- 1144 Gandolla, M., Ferrante, S., Baldassini, D., Cotti Cottini, M., Seneci, C., Molteni, F., et al. (2016a). EMG-  
1145 Controlled robotic hand rehabilitation device for domestic training. In *IFMBE Proceedings* (Springer  
1146 Verlag), vol. 57, 638–642. doi:10.1007/978-3-319-32703-7{\\_}124
- 1147 Gandolla, M., Ferrante, S., Molteni, F., Guanziroli, E., Frattini, T., Martegani, A., et al. (2014). Re-thinking  
1148 the role of motor cortex: Context-sensitive motor outputs? *NeuroImage* 91, 366–374. doi:10.1016/j.  
1149 neuroimage.2014.01.011
- 1150 Gandolla, M., Niero, L., Molteni, F., Guanziroli, E., Ward, N. S., and Pedrocchi, A. (2021). Brain  
1151 Plasticity Mechanisms Underlying Motor Control Reorganization: Pilot Longitudinal Study on Post-  
1152 Stroke Subjects. *Brain Sciences* 2021, Vol. 11, Page 329 11, 329. doi:10.3390/BRAINSCI11030329
- 1153 Gandolla, M., Ward, N. S., Molteni, F., Guanziroli, E., Ferrigno, G., and Pedrocchi, A. (2016b). The Neural  
1154 Correlates of Long-Term Carryover following Functional Electrical Stimulation for Stroke. *Neural  
1155 Plasticity* 2016. doi:10.1155/2016/4192718
- 1156 Guidali, M., Duschau-Wicke, A., Broggi, S., Klamroth-Marganska, V., Nef, T., and Riener, R. (2011).  
1157 A robotic system to train activities of daily living in a virtual environment. *Medical and Biological  
1158 Engineering and Computing* 49, 1213–1223. doi:10.1007/s11517-011-0809-0
- 1159 Gull, M. A., Bai, S., and Bak, T. (2020). A review on design of upper limb exoskeletons. *Robotics* 9, 1–35.  
1160 doi:10.3390/robotics9010016

- 1161 Hill, P. W., Wolbrecht, E. T., and Perry, J. C. (2019). Gravity compensation of an exoskeleton joint using  
1162 constant-force springs. *IEEE International Conference on Rehabilitation Robotics* 2019-June, 311–316.  
1163 doi:10.1109/ICORR.2019.8779422
- 1164 Hogan, N. (1985). Impedance control: An approach to manipulation: Part I-theory. *Journal of Dynamic*  
1165 *Systems, Measurement and Control, Transactions of the ASME* 107, 1–7. doi:10.1115/1.3140702
- 1166 Hong, K. S., Ghafoor, U., and Khan, M. J. (2020). Brain–machine interfaces using functional near-infrared  
1167 spectroscopy: a review. *Artificial Life and Robotics* 25, 204–218. doi:10.1007/s10015-020-00592-9
- 1168 Howlett, O. A., Lannin, N. A., Ada, L., and Mckinstry, C. (2015). Functional Electrical Stimulation  
1169 Improves Activity After Stroke: A Systematic Review With Meta-Analysis. *Archives of Physical*  
1170 *Medicine and Rehabilitation* 96, 934–943. doi:10.1016/J.APMR.2015.01.013
- 1171 Huang, V. S. and Krakauer, J. W. (2009). Robotic neurorehabilitation: A computational motor learning  
1172 perspective. *Journal of NeuroEngineering and Rehabilitation* 6, 5. doi:10.1186/1743-0003-6-5
- 1173 Iandolo, R., Marini, F., Semprini, M., Laffranchi, M., Mugnosso, M., Cherif, A., et al. (2019). Perspectives  
1174 and Challenges in Robotic Neurorehabilitation. *Applied Sciences* 9, 3183. doi:10.3390/app9153183
- 1175 [Dataset] Israely, S. and Carmeli, E. (2016). Error augmentation as a possible technique for improving  
1176 upper extremity motor performance after a stroke - A systematic review. doi:10.1179/1945511915Y.  
1177 0000000007
- 1178 [Dataset] Jarrassé, N., Proietti, T., Crocher, V., Robertson, O., Sahbani, A., Morel, G., et al. (2014). Robotic  
1179 exoskeletons: A perspective for the rehabilitation of arm coordination in stroke patients. doi:10.3389/  
1180 fnhum.2014.00947
- 1181 Just, F., Baur, K., Riener, R., Klamroth-Marganska, V., and Rauter, G. (2016). Online adaptive  
1182 compensation of the ARMin Rehabilitation Robot. *Proceedings of the IEEE RAS and EMBS International*  
1183 *Conference on Biomedical Robotics and Biomechatronics* 2016-July, 747–752. doi:10.1109/BIOROB.  
1184 2016.7523716
- 1185 Just, F., Ozen, O., Bosch, P., Bobrovsky, H., Klamroth-Marganska, V., Riener, R., et al. (2018). Exoskeleton  
1186 transparency: Feed-forward compensation vs. disturbance observer. *At-Automatisierungstechnik* 66,  
1187 1014–1026. doi:10.1515/auto-2018-0069
- 1188 Just, F., Ozen, O., Tortora, S., Klamroth-Marganska, V., Riener, R., and Rauter, G. (2020). Human  
1189 arm weight compensation in rehabilitation robotics: Efficacy of three distinct methods. *Journal of*  
1190 *NeuroEngineering and Rehabilitation* 17, 1–17. doi:10.1186/s12984-020-0644-3
- 1191 Just, F., Ozen, O., Tortora, S., Riener, R., and Rauter, G. (2017). Feedforward model based arm weight  
1192 compensation with the rehabilitation robot ARMin. *IEEE International Conference on Rehabilitation*  
1193 *Robotics* , 72–77doi:10.1109/ICORR.2017.8009224
- 1194 Kahn, L. E., Lum, P. S., Rymer, W. Z., and Reinkensmeyer, D. J. (2006a). Robot-assisted movement  
1195 training for the stroke-impaired arm: Does it matter what the robot does? *Journal of Rehabilitation*  
1196 *Research and Development* 43, 619–629. doi:10.1682/JRRD.2005.03.0056
- 1197 Kahn, L. E., Zygmant, M. L., Rymer, W. Z., and Reinkensmeyer, D. J. (2006b). Robot-assisted reaching  
1198 exercise promotes arm movement recovery in chronic hemiparetic stroke: A randomized controlled pilot  
1199 study. *Journal of NeuroEngineering and Rehabilitation* 3, 1–13. doi:10.1186/1743-0003-3-12
- 1200 Keemink, A. Q., van der Kooij, H., and Stienen, A. H. (2018). Admittance control for physical  
1201 human–robot interaction. *The International Journal of Robotics Research* 37, 1421–1444. doi:10.  
1202 1177/0278364918768950
- 1203 Khalil, W. and Dombre, E. (2002). Compliant motion control. In *Modeling, Identification and Control of*  
1204 *Robots* (Elsevier). 377–393. doi:10.1016/B978-190399666-9/50015-4

- 1205 Khan, H., Naseer, N., Yazidi, A., Eide, P. K., Hassan, H. W., and Mirtaheri, P. (2021). Analysis of Human  
1206 Gait Using Hybrid EEG-fNIRS-Based BCI System: A Review. *Frontiers in Human Neuroscience* 14,  
1207 605. doi:10.3389/fnhum.2020.613254
- 1208 Kim, B. and Deshpande, A. D. (2015). Controls for the shoulder mechanism of an upper-body exoskeleton  
1209 for promoting scapulohumeral rhythm. *IEEE International Conference on Rehabilitation Robotics*  
1210 2015-Septe, 538–542. doi:10.1109/ICORR.2015.7281255
- 1211 Kim, B. and Deshpande, A. D. (2017). An upper-body rehabilitation exoskeleton Harmony with  
1212 an anatomical shoulder mechanism: Design, modeling, control, and performance evaluation. *The*  
1213 *International Journal of Robotics Research* 36, 414–435. doi:10.1177/0278364917706743
- 1214 Kong, K., Moon, H., Jeon, D., and Tomizuka, M. (2010). Control of an exoskeleton for realization of  
1215 aquatic therapy effects. *IEEE/ASME Transactions on Mechatronics* 15, 191–200. doi:10.1109/TMECH.  
1216 2010.2041243
- 1217 Krakauer, J. W. (2006). Motor learning: its relevance to stroke recovery and neurorehabilitation. *Current*  
1218 *Opinion in Neurology* 19, 84–90. doi:10.1097/01.wco.0000200544.29915.cc
- 1219 [Dataset] Krebs, H. I., Palazzolo, J. J., Dipietro, L., Ferraro, M., Krol, J., Rannekleiv, K., et al.  
1220 (2003). Rehabilitation robotics: Performance-based progressive robot-assisted therapy. doi:10.1023/A:  
1221 1024494031121
- 1222 Kumar, S., Wöhrle, H., Trampler, M., Simnofske, M., Peters, H., Mallwitz, M., et al. (2019). Modular  
1223 design and decentralized control of the RECUPERA exoskeleton for stroke rehabilitation. *Applied*  
1224 *Sciences (Switzerland)* 9, 626. doi:10.3390/app9040626
- 1225 Langhorne, P., Coupar, F., and Pollock, A. (2009). Motor recovery after stroke: a systematic review. *The*  
1226 *Lancet Neurology* 8, 741–754. doi:10.1016/S1474-4422(09)70150-4
- 1227 Lin, C.-H., Lien, W.-M., Wang, W.-W., Chen, S.-H., Lo, C.-H., Lin, S.-Y., et al. (2014). NTUH-II robot  
1228 arm with dynamic torque gain adjustment method for frozen shoulder rehabilitation. In *2014 IEEE/RSJ*  
1229 *International Conference on Intelligent Robots and Systems (IEEE)*, 3555–3560. doi:10.1109/IROS.  
1230 2014.6943059
- 1231 Lin, Y., Qu, Q., Lin, Y., He, J., Zhang, Q., Wang, C., et al. (2021). Customizing Robot-Assisted Passive  
1232 Neurorehabilitation Exercise Based on Teaching Training Mechanism. *BioMed Research International*  
1233 2021. doi:10.1155/2021/9972560
- 1234 Lo, H. S. and Xie, S. Q. (2012). Exoskeleton robots for upper-limb rehabilitation: State of the art and future  
1235 prospects. *Medical Engineering and Physics* 34, 261–268. doi:10.1016/j.medengphy.2011.10.004
- 1236 Lum, P. S., Burgar, C. G., Van Der Loos, M., Shor, P. C., Majmundar, M., and Yap, R. (2006). MIME  
1237 robotic device for upper-limb neurorehabilitation in subacute stroke subjects: A follow-up study. *Journal*  
1238 *of Rehabilitation Research and Development* 43, 631–642. doi:10.1682/JRRD.2005.02.0044
- 1239 Maciejasz, P., Eschweiler, J., Gerlach-Hahn, K., Jansen-Troy, A., and Leonhardt, S. (2014). A survey on  
1240 robotic devices for upper limb rehabilitation. *Journal of NeuroEngineering and Rehabilitation* 11, 3.  
1241 doi:10.1186/1743-0003-11-3
- 1242 Marchal-Crespo, L. and Reinkensmeyer, D. J. (2009). Review of control strategies for robotic movement  
1243 training after neurologic injury. *Journal of NeuroEngineering and Rehabilitation* 6. doi:10.1186/  
1244 1743-0003-6-20
- 1245 Masiero, S., Celia, A., Rosati, G., and Armani, M. (2007). Robotic-Assisted Rehabilitation of the  
1246 Upper Limb After Acute Stroke. *Archives of Physical Medicine and Rehabilitation* 88, 142–149.  
1247 doi:10.1016/j.apmr.2006.10.032
- 1248 Mehdi, H. and Boubaker, O. (2012). Stiffness and Impedance Control Using Lyapunov Theory for  
1249 Robot-Aided Rehabilitation. *International Journal of Social Robotics* 4, 107–119. doi:10.1007/

- 1250 s12369-011-0128-5
- 1251 Mehrholz, J. (2019). Is Electromechanical and Robot-Assisted Arm Training Effective for Improving  
1252 Arm Function in People Who Have Had a Stroke?: A Cochrane Review Summary with Commentary.  
1253 *American Journal of Physical Medicine and Rehabilitation* 98, 339–340. doi:10.1097/PHM.  
1254 0000000000001133
- 1255 Miao, Q., Zhang, M., Cao, J., and Xie, S. Q. (2018). Reviewing high-level control techniques on robot-  
1256 assisted upper-limb rehabilitation. *Advanced Robotics* 32, 1253–1268. doi:10.1080/01691864.2018.  
1257 1546617
- 1258 Moubarak, S., Pham, M. T., Moreau, R., and Redarce, T. (2010). Gravity compensation of an upper  
1259 extremity exoskeleton. In *2010 Annual International Conference of the IEEE Engineering in Medicine  
1260 and Biology (IEEE)*, 4489–4493. doi:10.1109/IEMBS.2010.5626036
- 1261 Nef, T., Guidali, M., and Riener, R. (2009a). ARMin III - arm therapy exoskeleton with an ergonomic  
1262 shoulder actuation. *Applied Bionics and Biomechanics* 6, 127–142. doi:10.1080/11762320902840179
- 1263 Nef, T., Guidali, M., and Riener, R. (2009b). ARMin III-arm therapy exoskeleton with an ergonomic  
1264 shoulder actuation. *Applied Bionics and Biomechanics* 6, 127–142. doi:10.1080/11762320902840179
- 1265 Nef, T. and Lum, P. (2009). Improving backdrivability in geared rehabilitation robots. *Medical & Biological  
1266 Engineering & Computing* 47, 441–447. doi:10.1007/s11517-009-0437-0
- 1267 Nef, T., Mihelj, M., and Riener, R. (2007). ARMin: A robot for patient-cooperative arm therapy. *Medical  
1268 and Biological Engineering and Computing* 45, 887–900. doi:10.1007/s11517-007-0226-6
- 1269 Nicolas-Alonso, L. F. and Gomez-Gil, J. (2012). Brain computer interfaces, a review. *Sensors* 12,  
1270 1211–1279. doi:10.3390/s120201211
- 1271 Noda, T., Sugimoto, N., Furukawa, J., Sato, M. A., Hyon, S. H., and Morimoto, J. (2012). Brain-controlled  
1272 exoskeleton robot for BMI rehabilitation. *IEEE-RAS International Conference on Humanoid Robots* ,  
1273 21–27doi:10.1109/HUMANOIDS.2012.6651494
- 1274 Nordin, N., Xie, S. Q., and Wünsche, B. (2014). Assessment of movement quality in robot- Assisted upper  
1275 limb rehabilitation after stroke: A review. *Journal of NeuroEngineering and Rehabilitation* 11, 137.  
1276 doi:10.1186/1743-0003-11-137
- 1277 Novak, D. and Riener, R. (2013). Enhancing patient freedom in rehabilitation robotics using gaze-based  
1278 intention detection. In *2013 IEEE 13th International Conference on Rehabilitation Robotics (ICORR)*  
1279 (IEEE), 1–6. doi:10.1109/ICORR.2013.6650507
- 1280 Oldewurtel, F., Mihelj, M., Nef, T., and Riener, R. (2007). Patient-cooperative control strategies for  
1281 coordinated functional arm movements. In *2007 European Control Conference, ECC 2007 (IEEE)*,  
1282 2527–2534. doi:10.23919/ECC.2007.7068298
- 1283 Ostadabbas, S., Housley, S. N., Sebki, N., Richards, K., Wu, D., Zhang, Z., et al. (2016). Tongue-  
1284 controlled robotic rehabilitation: A feasibility study in people with stroke. *Journal of Rehabilitation  
1285 Research and Development* 53, 989–1006. doi:10.1682/JRRD.2015.06.0122
- 1286 Ott, C., Mukherjee, R., and Nakamura, Y. (2010). Unified impedance and admittance control. In  
1287 *Proceedings - IEEE International Conference on Robotics and Automation (IEEE)*, 554–561. doi:10.  
1288 1109/ROBOT.2010.5509861
- 1289 Patton, J. L., Stoykov, M. E., Kovic, M., and Mussa-Ivaldi, F. A. (2006). Evaluation of robotic training  
1290 forces that either enhance or reduce error in chronic hemiparetic stroke survivors. *Experimental Brain  
1291 Research* 168, 368–383. doi:10.1007/s00221-005-0097-8
- 1292 Pérez-Ibarra, J. C., Siqueira, A. A., Silva-Couto, M. A., De Russo, T. L., and Krebs, H. I. (2019). Adaptive  
1293 Impedance Control Applied to Robot-Aided Neuro-Rehabilitation of the Ankle. *IEEE Robotics and  
1294 Automation Letters* 4, 185–192. doi:10.1109/LRA.2018.2885165

- 1295 Perry, J. C., Maura, R., Bitikofer, C. K., and Wolbrecht, E. T. (2018). BLUE SABINO: Development of  
1296 a Bilateral Exoskeleton Instrument for Comprehensive Upper-Extremity Neuromuscular Assessment.  
1297 *Biosystems and Biorobotics* 21, 493–497. doi:10.1007/978-3-030-01845-0{\\_}99
- 1298 Péter, O., Fazekas, G., Zsiga, K., and Dénes, Z. (2011). Robot-mediated upper limb physiotherapy: Review  
1299 and recommendations for future clinical trials. *International Journal of Rehabilitation Research* 34,  
1300 196–202. doi:10.1097/MRR.0b013e328346e8ad
- 1301 Pignolo, L., Dolce, G., Basta, G., Lucca, L. F., Serra, S., and Sannita, W. G. (2012). Upper limb  
1302 rehabilitation after stroke: ARAMIS a "robo-mechatronic" innovative approach and prototype. In *2012*  
1303 *4th IEEE RAS & EMBS International Conference on Biomedical Robotics and Biomechanics (BioRob)*  
1304 (IEEE), 1410–1414. doi:10.1109/BioRob.2012.6290868
- 1305 Pignolo, L., Lucca, L. L., Basta, G., Serra, S., Pugliese, M. E., Sannita, W. G., et al. (2016). A new  
1306 treatment in the rehabilitation of the paretic upper limb after stroke: the ARAMIS prototype and treatment  
1307 protocol. *Ann Ist Super Sanità* 52, 301–308. doi:10.4415/ANN160225
- 1308 Pirondini, E., Coscia, M., Marcheschi, S., Roas, G., Salsedo, F., Frisoli, A., et al. (2016). Evaluation  
1309 of the effects of the Arm Light Exoskeleton on movement execution and muscle activities: a pilot  
1310 study on healthy subjects. *Journal of NeuroEngineering and Rehabilitation* 13, 9. doi:10.1186/  
1311 s12984-016-0117-x
- 1312 Proietti, T., Crocher, V., Roby-Brami, A., and Jarrasse, N. (2016). Upper-limb robotic exoskeletons for  
1313 neurorehabilitation: A review on control strategies. *IEEE Reviews in Biomedical Engineering* 9, 4–14.  
1314 doi:10.1109/RBME.2016.2552201
- 1315 Proietti, T., Guigon, E., Roby-Brami, A., and Jarrassé, N. (2017). Modifying upper-limb inter-joint  
1316 coordination in healthy subjects by training with a robotic exoskeleton. *Journal of NeuroEngineering*  
1317 *and Rehabilitation* 2017 14:1 14, 1–19. doi:10.1186/S12984-017-0254-X
- 1318 Proietti, T., Jarrassé, N., Roby-Brami, A., and Morel, G. (2015). Adaptive control of a robotic exoskeleton  
1319 for neurorehabilitation. In *International IEEE/EMBS Conference on Neural Engineering, NER* (IEEE),  
1320 vol. 2015-July, 803–806. doi:10.1109/NER.2015.7146745
- 1321 Puchinger, M., Kurup, N. B. R., Keck, T., Zajc, J., Russold, M. F., and Gföhler, M. (2018). The Retrainer  
1322 Light-Weight Arm Exoskeleton: Effect of Adjustable Gravity Compensation on Muscle Activations and  
1323 Forces. *Proceedings of the IEEE RAS and EMBS International Conference on Biomedical Robotics and*  
1324 *Biomechanics* 2018-Augus, 396–401. doi:10.1109/BIOROB.2018.8487218
- 1325 Ragonesi, D., Agrawal, S. K., Sample, W., and Rahman, T. (2013). Quantifying anti-gravity torques for the  
1326 design of a powered exoskeleton. *IEEE Transactions on Neural Systems and Rehabilitation Engineering*  
1327 21, 283–288. doi:10.1109/TNSRE.2012.2222047
- 1328 Rehmat, N., Zuo, J., Meng, W., Liu, Q., Xie, S. Q., and Liang, H. (2018). Upper limb rehabilitation using  
1329 robotic exoskeleton systems: a systematic review. *International Journal of Intelligent Robotics and*  
1330 *Applications* 2, 283–295. doi:10.1007/s41315-018-0064-8
- 1331 Reinkensmeyer, D. J., Burdet, E., Casadio, M., Krakauer, J. W., Kwakkel, G., Lang, C. E., et al. (2016).  
1332 Computational neurorehabilitation: modeling plasticity and learning to predict recovery. *Journal of*  
1333 *NeuroEngineering and Rehabilitation* 13, 42. doi:10.1186/s12984-016-0148-3
- 1334 Rodgers, H., Bosomworth, H., Krebs, H. I., van Wijck, F., Howel, D., Wilson, N., et al. (2019). Robot  
1335 assisted training for the upper limb after stroke (RATULS): a multicentre randomised controlled trial.  
1336 *The Lancet* 394, 51–62. doi:10.1016/S0140-6736(19)31055-4
- 1337 Sanchez, R. J., Wolbrecht, E., Smith, R., Liu, J., Rao, S., Cramer, S., et al. (2005). A pneumatic robot for re-  
1338 training arm movement after stroke: Rationale and mechanical design. *Proceedings of the 2005 IEEE 9th*  
1339 *International Conference on Rehabilitation Robotics* 2005, 500–504. doi:10.1109/ICORR.2005.1501151

- 1340 Schumacher, M., Wojtusich, J., Beckerle, P., and von Stryk, O. (2019). An introductory review of active  
1341 compliant control. *Robotics and Autonomous Systems* 119, 185–200. doi:10.1016/j.robot.2019.06.009
- 1342 Shadmehr, R., Smith, M. A., and Krakauer, J. W. (2010). Error correction, sensory prediction,  
1343 and adaptation in motor control. *Annual Review of Neuroscience* 33, 89–108. doi:10.1146/  
1344 annurev-neuro-060909-153135
- 1345 Shen, Y., Ma, J., Dobkin, B., and Rosen, J. (2018). Asymmetric Dual Arm Approach for Post Stroke  
1346 Recovery of Motor Functions Utilizing the EXO-UL8 Exoskeleton System: A Pilot Study. In *Proceedings*  
1347 *of the Annual International Conference of the IEEE Engineering in Medicine and Biology Society, EMBS*  
1348 (Institute of Electrical and Electronics Engineers Inc.), vol. 2018-July, 1701–1707. doi:10.1109/EMBC.  
1349 2018.8512665
- 1350 Shen, Y., Sun, J., Ma, J., and Rosen, J. (2019). Admittance Control Scheme Comparison of EXO-UL8: A  
1351 Dual-Arm Exoskeleton Robotic System. In *2019 IEEE 16th International Conference on Rehabilitation*  
1352 *Robotics (ICORR)* (IEEE), vol. 2019-June, 611–617. doi:10.1109/ICORR.2019.8779545
- 1353 Soltani-Zarrin, R., Zeiaee, A., Eib, A., Langari, R., Robson, N., and Tafreshi, R. (2018). TAMU  
1354 CLEVERarm: A novel exoskeleton for rehabilitation of upper limb impairments. In *2017 International*  
1355 *Symposium on Wearable Robotics and Rehabilitation, WeRob 2017* (Institute of Electrical and Electronics  
1356 Engineers Inc.), 1–2. doi:10.1109/WEROB.2017.8383844
- 1357 Soltani-Zarrin, R., Zeiaee, A., Langari, R., and Robson, N. (2017). Reference path generation for upper-arm  
1358 exoskeletons considering scapulohumeral rhythms. *IEEE International Conference on Rehabilitation*  
1359 *Robotics*, 753–758doi:10.1109/ICORR.2017.8009338
- 1360 Song, Z., Guo, S., Pang, M., Zhang, S., Xiao, N., Gao, B., et al. (2014). Implementation of resistance  
1361 training using an upper-limb exoskeleton rehabilitation device for elbow joint. *Journal of Medical and*  
1362 *Biological Engineering* 34, 188–196. doi:10.5405/jmbe.1337
- 1363 Stroppa, F., Loconsole, C., Marcheschi, S., and Frisoli, A. (2017a). A Robot-Assisted Neuro-Rehabilitation  
1364 System for Post-Stroke Patients’ Motor Skill Evaluation with ALEx Exoskeleton. In *Biosystems and*  
1365 *Biorobotics* (Springer, Cham), vol. 15. 501–505. doi:10.1007/978-3-319-46669-9{\\_}83
- 1366 Stroppa, F., Loconsole, C., Marcheschi, S., Mastronicola, N., and Frisoli, A. (2018). An Improved  
1367 Adaptive Robotic Assistance Methodology for Upper-Limb Rehabilitation. In *Lecture Notes in Computer*  
1368 *Science (including subseries Lecture Notes in Artificial Intelligence and Lecture Notes in Bioinformatics)*  
1369 (Springer, Cham), vol. 10894 LNCS, 513–525. doi:10.1007/978-3-319-93399-3{\\_}44
- 1370 Stroppa, F., Marcheschi, S., Mastronicola, N., Loconsole, C., and Frisoli, A. (2017b). Online adaptive  
1371 assistance control in robot-based neurorehabilitation therapy. In *IEEE International Conference on*  
1372 *Rehabilitation Robotics* (IEEE Computer Society), 628–633. doi:10.1109/ICORR.2017.8009318
- 1373 Trigili, E., Crea, S., Moisè, M., Baldoni, A., Cempini, M., Ercolini, G., et al. (2020). Design and  
1374 experimental characterization of a shoulder-elbow exoskeleton with compliant joints for post-stroke  
1375 rehabilitation. *IEEE/ASME Transactions on Mechatronics* 24, 1485–1496. doi:10.1109/TMECH.2019.  
1376 2907465
- 1377 Vallery, H., Veneman, J., van Asseldonk, E., Ekkelenkamp, R., Buss, M., and van Der Kooij, H. (2008).  
1378 Compliant actuation of rehabilitation robots. *IEEE Robotics and Automation Magazine* 15, 60–69.  
1379 doi:10.1109/MRA.2008.927689
- 1380 Van Delden, A. E., Peper, C. E., Kwakkel, G., and Beek, P. J. (2012). A systematic review of bilateral  
1381 upper limb training devices for poststroke rehabilitation. *Stroke Research and Treatment* doi:10.1155/  
1382 2012/972069
- 1383 Veerbeek, J. M., Langbroek-Amersfoort, A. C., Van Wegen, E. E., Meskers, C. G., and Kwakkel, G. (2017).  
1384 Effects of Robot-Assisted Therapy for the Upper Limb after Stroke. *Neurorehabilitation and Neural*

- 1385 *Repair* 31, 107–121. doi:10.1177/1545968316666957
- 1386 Villani, L. and De Schutter, J. (2008). Force Control. In *Springer Handbook of Robotics* (Springer Berlin  
1387 Heidelberg). 161–185. doi:10.1007/978-3-540-30301-5{\\_}8
- 1388 Wang, J. and Barry, O. R. (2021). Inverse Optimal Robust Adaptive Controller for Upper Limb  
1389 Rehabilitation Exoskeletons with Inertia and Load Uncertainties. *IEEE Robotics and Automation*  
1390 *Letters* 6, 2171–2178. doi:10.1109/LRA.2021.3061361
- 1391 Weiss, P., Zenker, P., and Maehle, E. (2012). Feed-forward friction and inertia compensation for improving  
1392 backdrivability of motors. In *2012 12th International Conference on Control, Automation, Robotics and*  
1393 *Vision, ICARCV 2012*. 288–293. doi:10.1109/ICARCV.2012.6485173
- 1394 Winter, D. A. (2009). Kinetics: Forces and Moments of Force. In *Biomechanics and Motor Control of*  
1395 *Human Movement* (John Wiley & Sons, Inc.). 107–138. doi:10.1002/9780470549148.ch5
- 1396 Wolbrecht, E. T., Chan, V., Reinkensmeyer, D. J., and Bobrow, J. E. (2008). Optimizing compliant,  
1397 model-based robotic assistance to promote neurorehabilitation. *IEEE Transactions on Neural Systems*  
1398 *and Rehabilitation Engineering* 16, 286–297. doi:10.1109/TNSRE.2008.918389
- 1399 Wright, Z. A., Lazzaro, E., Thielbar, K. O., Patton, J. L., and Huang, F. C. (2018). Robot Training with  
1400 Vector Fields Based on Stroke Survivors' Individual Movement Statistics. *IEEE Transactions on Neural*  
1401 *Systems and Rehabilitation Engineering* 26, 307–323. doi:10.1109/TNSRE.2017.2763458
- 1402 Wright, Z. A., Patton, J. L., Huang, F. C., and Lazzaro, E. (2015). Evaluation of force field training  
1403 customized according to individual movement deficit patterns. *IEEE International Conference on*  
1404 *Rehabilitation Robotics* 2015-Sept, 193–198. doi:10.1109/ICORR.2015.7281198
- 1405 Wu, J., Cheng, H., Zhang, J., Yang, S., and Cai, S. (2021). Robot-Assisted Therapy for Upper Extremity  
1406 Motor Impairment after Stroke: A Systematic Review and Meta-Analysis. *Physical Therapy* 101.  
1407 doi:10.1093/ptj/pzab010
- 1408 Wu, K. Y., Su, Y. Y., Yu, Y. L., Lin, C. H., and Lan, C. C. (2019). A 5-Degrees-of-Freedom Lightweight  
1409 Elbow-Wrist Exoskeleton for Forearm Fine-Motion Rehabilitation. *IEEE/ASME Transactions on*  
1410 *Mechatronics* 24, 2684–2695. doi:10.1109/TMECH.2019.2945491
- 1411 Wu, Q., Wang, X., Chen, B., and Wu, H. (2018a). Development of a Minimal-Intervention-Based  
1412 Admittance Control Strategy for Upper Extremity Rehabilitation Exoskeleton. *IEEE Transactions on*  
1413 *Systems, Man, and Cybernetics: Systems* 48, 1005–1016. doi:10.1109/TSMC.2017.2771227
- 1414 Wu, Q., Wang, X., Chen, B., and Wu, H. (2018b). Patient-active control of a powered exoskeleton targeting  
1415 upper limb rehabilitation training. *Frontiers in Neurology* 9, 817. doi:10.3389/fneur.2018.00817
- 1416 Xu, G., Song, A., and Li, H. (2011). Control system design for an upper-limb rehabilitation robot.  
1417 *Advanced Robotics* 25, 229–251. doi:10.1163/016918610X538561
- 1418 Zeiaee, A., Soltani-Zarrin, R., Langari, R., and Tafreshi, R. (2019). Kinematic Design Optimization  
1419 of an Eight Degree-of-Freedom Upper-Limb Exoskeleton. *Robotica* 37, 2073–2086. doi:10.1017/  
1420 S0263574719001085
- 1421 Zhang, L., Guo, S., and Sun, Q. (2020). An Assist-as-Needed Controller for Passive, Assistant, Active,  
1422 and Resistive Robot-Aided Rehabilitation Training of the Upper Extremity. *Applied Sciences* 11, 340.  
1423 doi:10.3390/app11010340
- 1424 Zhuang, Y., Yao, S., Ma, C., and Song, R. (2019). Admittance Control Based on EMG-Driven  
1425 Musculoskeletal Model Improves the Human-Robot Synchronization. *IEEE Transactions on Industrial*  
1426 *Informatics* 15, 1211–1218. doi:10.1109/TII.2018.2875729